Master's thesis

NTNU
Norwegian University of Science and Technology
Faculty of Natural Sciences
Department of Chemistry

Tor Strømsem Haugland

Modeling Chemistry in QED Cavities using Coupled Cluster

Master's thesis in Applied Theoretial Chemistry
Supervisor: Henrik Koch
June 2019

NTNU
Norwegian University of
Science and Technology

Modeling Chemistry in QED Cavities using Coupled Cluster

Tor Strømsem Haugland

Supervisor *Prof. Henrik Koch*

Co-Supervisor *Enrico Ronca*

Co-Supervisor *Eirik Fadum Kjønstad*

June 21, 2019

NTNU

Rest of this page intentionally left blank.

Sammendrag

I denne avhandlingen introduseres kvanteelektrodynamisk "coupled cluster" teori (QED-CC) som en ny og nøyaktig *ab initio* teori for å undersøke sterk kobling mellom lys og materie i optiske kaviteter. Ligningene for grunntilstand og eksiterte tilstander for QED-CC blir bestemt ved hjelp av Pauli-Fierz Hamiltonoperatoren og "koherente" fotontilstander. Kvanteelektrodynamisk Hartree-Fock teori (QED-HF) er utledet som referansebølgefunksjon for QED-CC. Ved å bruke pertubasjonsteori kan det argumenteres for at de koblede dobbelt amplitudene er små, som forenkler QED-CCSD ligningene. Vi presenterer en implementering av grunntilstander og eksiterte tilstander for QED-CCS og QED-CCSD. Ved å sammenligne disse med en eksakt referansetilstand, ser man at QED-CCSD er i stand til å reprodusere egenskaper til lys-masse systemet ved sterke koblinger for de to små testmolekylene H_2 og HF. Bruk av QED-CCSD for realistiske molekyler blir demonstrert ved å studere p-nitroanilin (PNA) i en kavitet som er i ressonans med molekylets "charge transfer" tilstand, som har en stor Rabi-splitting (1.22 eV) ved sterke koblinger ($\lambda = 0.05$). QED-CC åpner opp mulighetene for å undersøke nye retninger innenfor kavitet-elektrodynamikk, inkludert forståelsen av fundamentale egenskaper av koblede elektron-foton system, modifisert reaktivitet i sterk lys-materie kobling og lang-distanse effekter fra sammenfiltrerte fotoner.

Rest of this page intentionally left blank.

Abstract

In this thesis, we introduce quantum electrodynamical coupled cluster theory (QED-CC) as a new and accurate *ab initio* theory to investigate strong light-matter coupling in optical cavities. Starting from the Pauli-Fierz Hamiltonian in the long wavelength limit we establish the ground and excited state equations for QED-CC using coherent photon states. Quantum electrodynamical Hartree-Fock theory (QED-HF) was developed as a reference wavefunction for QED-CC. Perturbation theory is used to argue that the coupled doubles amplitudes are small, simplifying the QED-CCSD equations. We present an implementation of QED-CCS and QED-CCSD ground and excited states. A comparison to an exact reference shows that QED-CCSD reproduces the features of strong light-matter coupling for two small test molecules, H_2 and HF. We demonstrate that QED-CCSD can also be used for realistic molecules, which in our case is p-nitroaniline (PNA) in a cavity resonant with PNA's charge transfer state. The charge transfer state has a large Rabi splitting (1.22 eV) at strong couplings ($\lambda = 0.05$). QED-CC opens up the possibility of pursuing new directions in cavity quantum electrodynamics, including the understanding of the fundamentals of correlated electron-photon systems, modified reactivity in strong light-matter interaction, and long-range effects from entangled photons.

Rest of this page intentionally left blank.

Preface

This thesis was performed at and submitted to the "Norwegian University of Science and Technology" (NTNU), Department of Chemistry, and concludes the master's degree programme in Chemistry (MSCHEM) with specialization in applied theoretical chemistry. The present work was carried out between August 2018 and June 2019, supervised by Prof. Henrik Koch with co-supervisors Enrico Ronca and Eirik Kjønstad.

Rest of this page intentionally left blank.

Acknowledgements

I would like to thank my supervisor Professor Henrik Koch, who has inspired and instructed me in the study of *ab initio* chemistry. His passion for this field is unmatched, and I would like to thank him for both his patience and interest in my project. This project would not be possible without Enrico Ronca, who alongside Henrik, proposed this project to me. Enrico deserves praise for how many long hours he has spent with me, discussing various aspects of cavities and light-matter interaction. I am especially grateful for how much he has taught me about academic writing, which will become very useful for future papers. A special thanks goes to Eirik Kjønstad, who has been instrumental to the implementation of my project, both in terms of theory and implementation.

Finally I would like to thank my family and loved ones. To my parents, Lars & Hege, thank you for always being there for me. To Tonje and my little sister Stine, both of you deserve an especially big thanks for your love and support during this last year. Thank you.

Rest of this page intentionally left blank.

Contents

Rest of this page intentionally left blank.

Illustrative Elements

List of Figures

List of Tables

Chapter 1

Introduction

Manipulating matter using strong light-matter coupling creates new and interesting properties, while at the same time modifying already existing ones. Basov *et al.* has discussed the possibility of creating material properties on demand with strong light-matter interaction[1], which would allow for the systematic creation of materials exploiting quantum properties. This has caused a large growth in exploring both the theory and application of the strong light-matter interaction. Molecules coupled strongly to light have been used to inhibit[2], catalyze[3] and change selectivity[4] of chemical reactions, modify excitation- and charge transfers reactions[5, 6] and manipulate of photoisomerization[7]. In condensed matter physics, strong light-matter coupling has been used to create exciton-polaritons condensates[8, 9], modify superconductivity[10, 11] and induce phase transitions[12, 13] to name a few.

There are mainly two ways of coupling light and matter. The first approach is using intense classical lasers, which can form combined light-matter states by means of the AC Stark effect[14]. These light-matter states are known as *Floquet states*, and they have properties very different from purely electronic states that be utilized in new and exciting applications[12]. The disadvantage of using intense lasers to induce light-matter coupling is that the laser pushes the system out of equilibrium, reducing our ability to control the new properties. The other approach to light-matter coupling is *cavity quantum electrodynamics* (cavity QED), where optical cavities are used instead of lasers. Matter can couple to the quantized light inside a cavity, forming a combined light-matter state known as a *polariton*[15]. Even the vacuum state inside a cavity couples to matter, allowing us to study polaritons in the absence of photons.

In this thesis we delve into cavity QED, using optical cavities to induce light-matter interaction. An optical cavity is a set of highly reflective mirrors placed such that light circulates back and forth several times before dispersion effects come into play. In the simplest case, we have the Fabry-Perot resonator, where light circulates between two plane-parallel mirrors[16]. Here light acts as a harmonic oscillator with quantized frequencies determined by the distance between the mirrors. Interactions between matter and this quantized light generate hybrid light-matter states called *polaritons*.

Tuning the frequency of light, amount of photons and coupling strength produces new properties in matter such as new potential energy surfaces, including modifications to the already existing potential energy landscape.

Many model systems have been developed since the famous Jaynes-Cummings model[17] in 1963 to describe the interesting properties of strong light-matter interaction. The recent growth of cavity QED can be attributed to the improved quality of the optical cavities, allowing for much larger couplings than previously possible and even generate polaritons at room-temperature[18, 19]. Some recently used cavity types are plasmonic cavities[18, 20], metamaterials[21] and photonic crystals[22]. With the recent improvement in cavities, theories developed from quantum optics can now be tested and applied to experiments. However, there is still much room for improvement. While the frequency of light inside the cavity can easily be adjusted, the coupling strength is far more difficult to adjust. Reaching ultra-strong coupling has also proven itself to be very difficult in general.

Quantum chemistry is an established field dedicated to solve the Schrödinger equation and gain insight into molecular systems. Only the hydrogen atom has an analytical solution, while atoms and molecules with multiple electrons can only be solved "exactly" within a truncated basis. This is done with full configuration-interaction(FCI)[23], which has exponential scaling and can only be used on very small systems. Today, FCI is mostly used for testing and benchmarks[24–26]. Coupling photons with FCI will quickly make the problem computationally intractable, even for hydrogen in a truncated photon space. Coupled cluster (CC) has become the most successful model to accurately describe a molecular system with wavefunctions[23]. One of the first implementation of CC for practical use came in the 1980s with CCSD, where excitations were limited to singles and doubles[27]. Today, the CC models show great popularity and accuracy, and CCSD(T)[28] is known as the "gold standard" of quantum chemistry. Another approach to quantum chemistry, which has had immense success, is *density functional theory* (DFT), for which there exists numerous reviews[29, 30]. DFT uses electron densities instead of wavefunctions to calculate properties, reducing the dimensionality of the problem down to just 3 spatial coordinates.

The challenge of developing an *ab initio* model to accurately and efficiently compute the properties and chemistry of polaritons is still an open challenge. A semi-empirical model system was recently developed to describe the change in the photochemistry of azobenzene in a cavity[7], the Bethe-Salpeter equation was used to study exciton-polaritons in a 2D material inside a cavity[9], and variational theory beyond the dipole approximation[31] to name a few. Today, the only *ab initio* quantum chemistry method to add QED photons to molecules is QEDFT[32–34]. In QEDFT, electrons and photons are treated as independent particles and interact via the exchange-correlation functional. The biggest limitation of QEDFT is finding an accurate functional, which can describe both the electrons and the photons to sufficient accuracy. The current implementation of QEDFT with optimized effective potentials (OEP) works well at strong couplings but struggles at very strong couplings where two-photon processes

become important[35].

Due to the success of CC on electronic states, we wish to extend CC to cavity QED. In this thesis, we will present the first *ab initio* theory for molecules in an optical cavity using coupled cluster. We will start by presenting cavity QED and CC separately before we combine them into QED-CC. Most of the thesis will be theoretical, but we will apply a QED-CCSD program to calculate some features of the polaritonic states.

Rest of this page intentionally left blank.

Chapter 2

Quantum Electrodynamics and Cavities

In this chapter quantum electrodynamics is introduced from the classical electromagnetic field within an optical cavity. We then show how the quantized field couples to matter, generating the *polariton* light-matter states.

2.1 Quantized Electromagnetic Fields

To understand the interaction between a molecule and the electromagnetic field in a cavity we will first consider just the electromagnetic field. We will derive the Hamiltonian for the classical electromagnetic field, before we extend the equations to the quantum electromagnetic field.

Maxwell equations for an electromagnetic field without any currents, charges nor a dielectric media are[36]

$$\begin{aligned} \nabla \cdot \vec{\mathbf{E}} = 0\,, \quad \nabla \times \vec{\mathbf{E}} = \frac{\partial \vec{\mathbf{B}}}{\partial t}\,, \\ \nabla \cdot \vec{\mathbf{B}} = 0\,, \quad \nabla \times \vec{\mathbf{B}} = \mu_0 \epsilon_0 \frac{\partial \vec{\mathbf{E}}}{\partial t}\,. \end{aligned} \tag{2.1}$$

Let $\vec{\mathbf{E}}$ be an electric-field polarized along the x-direction,

$$\vec{\mathbf{E}}(\vec{\mathbf{r}}, t) = \hat{\mathbf{e}}_x E_x(z, t)\,. \tag{2.2}$$

where $\vec{\mathbf{r}} = (x, y, z)$ is the position vector. Consider this electric field inside a perfectly conducting cavity with boundary conditions $\vec{\mathbf{E}}(\vec{\mathbf{r}}, t) = 0$ when $z = 0$ and $z = L$ as visualized in Figure 2.1. The electric field for a single mode along the x-direction in the cavity is

$$E_x(z, t) = \sqrt{\frac{2\omega^2}{V\epsilon_0}} q(t) \sin(kz)\,, \tag{2.3}$$

where ω is the frequency of the mode, V is the volume of the cavity and k is the wave number $\omega = kc$. $q(t)$ is a function describing the time evolution of the electric field. To satisfy the boundary condition, k becomes quantized to $k = n\pi/L$ where $n = 1, 2, \ldots$. We emphasize that already in the classical case the electromagnetic field is quantized inside a cavity. The corresponding magnetic field can be found from Maxwells equations, Eq. [2.1], $\vec{\mathbf{B}} = \hat{\mathbf{e}}_y B_y(z,t)$ where B_y is

$$B_y(z,t) = \frac{\mu_0 \epsilon_0}{k} \sqrt{\frac{2\omega^2}{V\epsilon_0}} \dot{q}(t) \cos(kz) \,. \tag{2.4}$$

The Hamiltonian for a classical electromagnetic field is

$$\begin{aligned} H &= \frac{1}{2} \int \left(\epsilon_0 \|\mathbf{E}\|^2 + \mu_0^{-1} \|\mathbf{B}\|^2 \right) \mathrm{d}V \,, \\ &= \frac{1}{2} \left(\frac{2\epsilon_0}{V\epsilon_0} \right) \left(\omega^2 q^2 \int \sin^2(kz)\, \mathrm{d}V + \frac{\epsilon_0 \mu_0 \omega^2}{k^2} \dot{q}^2 \int \cos^2(kz)\, \mathrm{d}V \right) , \\ &= \frac{1}{V} \left(\omega^2 q^2 \frac{V}{2} + (\epsilon_0 \mu_0 c^2) \dot{q}^2 \frac{V}{2} \right) , \\ &= \frac{1}{2} (\dot{q}^2 + \omega^2 q^2) \,. \end{aligned} \tag{2.5}$$

Here we have used $c^2 = (\epsilon_0 \mu_0)^{-1}$. Recognizing q and $p = \dot{q}$ as the canonical position and momentum of the system simplifies the Hamiltonian to that of a harmonic oscillator,

$$H = \frac{1}{2} (p^2 + \omega^2 q^2) \,. \tag{2.6}$$

Going from classical to quantum is as simple as changing q and p to $\hat{q}$ and $\hat{p}$,

$$\hat{H} = \frac{1}{2} (\hat{p}^2 + \omega^2 \hat{q}^2) \,, \tag{2.7}$$

where $\hat{q}$ and $\hat{p}$ satisfies the *canonical commutation relation*,

$$[\hat{q}, \hat{p}] = i \,. \tag{2.8}$$

The solution to the harmonic oscillator is most conveniently done by introducing the photon annihilation operator $\hat{b}$ and the photon creation operator $\hat{b}^\dagger$, which are defined in terms of $\hat{q}$ and $\hat{p}$,

$$\hat{b}^\dagger = \sqrt{\frac{1}{2\omega}} (\omega \hat{q} + i\hat{p}) \,, \quad \hat{b} = \sqrt{\frac{1}{2\omega}} (\omega \hat{q} - i\hat{p}) \,. \tag{2.9}$$

From the canonical commutation relation [2.8], $\hat{b}^\dagger$ and $\hat{b}$ must satisfy the *boson commutation relation*,

$$\left[\hat{b}, \hat{b}^\dagger \right] = 1 \,. \tag{2.10}$$

This further simplifies the Hamiltonian [2.7] to

$$\hat{H} = \omega \hat{b}^\dagger \hat{b} + \frac{1}{2}\omega \,. \qquad [2.11]$$

Letting $\hat{b}^\dagger$ and $\hat{b}$ act on a photon number state creates and annihilates a photon respectively,

$$\hat{b}^\dagger |n\rangle = \sqrt{n+1}\,|n+1\rangle \,, \quad \hat{b}\,|n\rangle = \sqrt{n}\,|n-1\rangle \,. \qquad [2.12]$$

We can easily show that $\hat{H}$ is diagonal in the photon number states $|n\rangle$,

$$\langle n|\hat{H}|n\rangle = \omega\left(n + \frac{1}{2}\right), \quad \langle n|\hat{H}|m\rangle = 0 \,. \qquad [2.13]$$

For $n = 0$ we have the zero-point energy, $\frac{1}{2}\omega$, coming from vacuum fluctuations in the electromagnetic field. The zero-point energy does not show up in the classical field calculation, and is purely a property of quantum mechanics. In this derivation, we have limited ourselves to one photon mode. Since there is no interaction between the photons with different frequency and polarization, the full Hamiltonian with all photon modes is additive,

$$\hat{H} = \sum_\alpha \left(\omega_\alpha \hat{b}_\alpha^\dagger \hat{b}_\alpha + \frac{1}{2}\omega_\alpha\right). \qquad [2.14]$$

This Hamiltonian does not contain the volume of the cavity. We may freely stretch the cavity to become infinitely big, describing free space instead of just a cavity.

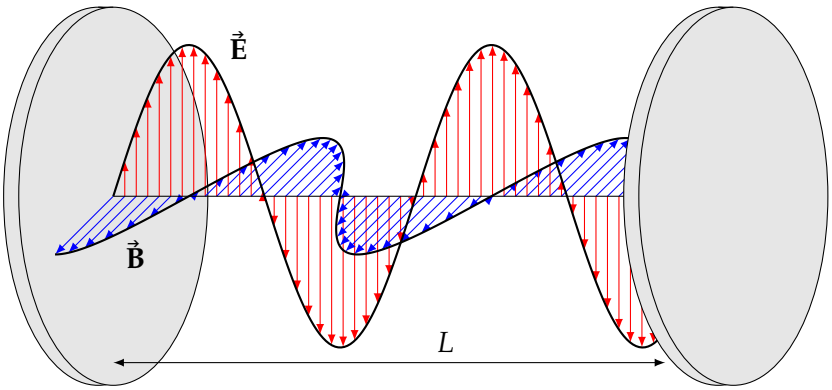

Figure 2.1 / Electric field $\vec{\mathbf{E}}$ and magnetic field $\vec{\mathbf{B}}$ inside a perfectly conductive cavity of length L.

2.1.1 Coherent States

The electric field operator can be written in terms of the annihilation and creation operators[36],

$$\hat{E}_x(\vec{\mathbf{r}},t) = \frac{1}{2} i \sqrt{\frac{2\omega}{V\epsilon_0}} (\hat{b} e^{i(\vec{\mathbf{k}}\cdot\vec{\mathbf{r}}-\omega t)} - \hat{b}^\dagger e^{-i(\vec{\mathbf{k}}\cdot\vec{\mathbf{r}}-\omega t)}) \,. \tag{2.15}$$

The average electric field over a Fock state is zero,

$$\langle n|\hat{E}_x(\vec{\mathbf{r}},t)|n\rangle = 0 \,. \tag{2.16}$$

This photon number states does not represent the field realistically in the limit of many photons, where we know that the electric field should represent the classic result with the possibility of being non-zero. One wavefunction that reproduces the classical result in the limit of many photons turns out to be the eigenstates of $\hat{b}$, the coherent states[36]. The displacement operator is defined as

$$\hat{D}(z) = e^{z\hat{b}^\dagger - z^*\hat{b}} \,. \tag{2.17}$$

Coherent states are generated from acting the displacement operator on the vacuum state,

$$|z\rangle = \hat{D}(z)\,|0\rangle \,. \tag{2.18}$$

We also have the generalized coherent states[37, 38], which are generated from acting the displacement operator on the photon number states,

$$|z,n\rangle = \hat{D}(z)\,|n\rangle \,. \tag{2.19}$$

The coherent state has a non-zero electric field,

$$\langle z|\hat{E}_x(\vec{\mathbf{r}},t)|z\rangle = \sqrt{\frac{2\omega}{V\epsilon_0}} \cdot |z| \sin\Big(\omega t - \vec{\mathbf{k}}\cdot\vec{\mathbf{r}} - \theta\Big) \,, \tag{2.20}$$

where we have written z in its polar form, $z = |z|e^{i\theta}$. The time-evolution of a coherent state for the harmonic oscillator Hamiltonian reproduces the classical result of a sinusoidal wave. Coherent states have many more interesting properties we will not delve into here[36].

2.2 Light-Matter Interaction

2.2.1 Hamiltonian

The non-relativistic minimal coupling Hamiltonian which describes the interaction between nuclei, electrons and the electromagnetic field is given by the Pauli-Fierz Hamil-

tonian[39]. Here we give the Hamiltonian in the Born-Oppenheimer approximation with one photon mode in the Coulomb gauge[40],

$$\hat{H} = \frac{1}{2}\sum_{j}^{N_e}\left(-\hat{\mathbf{p}}_j - \frac{e}{c}\hat{\mathbf{A}}(\hat{\mathbf{r}}_\mathbf{j})\right)^2 + \hat{V}_{ee} + \hat{V}_{en} + V_{nn}\,, \tag{2.21}$$

where N_e is the number of electrons, e is the electron charge, $\hat{\mathbf{p}}_j$ and $\hat{\mathbf{r}}_j$ is the momentum and position of the j-th electron. $\hat{V}_{ee}$, $\hat{V}_{en}$ and V_{nn} is the electron-electron, electron-nuclei and nuclei-nuclei interactions. $\hat{\mathbf{A}}$ is the vector potential,

$$\hat{\mathbf{A}}(\hat{\mathbf{r}}_j) = \frac{\lambda c}{\sqrt{2\omega}}\vec{\boldsymbol{\epsilon}}(\hat{b}^\dagger e^{i\vec{\mathbf{k}}\cdot\vec{\mathbf{r}}_j} + \hat{b}e^{-i\vec{\mathbf{k}}\cdot\vec{\mathbf{r}}_j})\,, \tag{2.22}$$

where $\lambda = \sqrt{\frac{4\pi}{V}}$ is the coupling strength. The wavelength of the photon required to excite the molecule is often much larger than the size of the molecule. In a majority of cases we are in the long wavelength limit, also known as the dipole approximation,

$$e^{i\vec{\mathbf{k}}\cdot\vec{\mathbf{r}}} \approx 1\,. \tag{2.23}$$

In practice, this means that the entire molecule "feels" the same field. For molecules at the size of Ångströms, we are limited to UV-light and up. We can insert the dipole approximation, [2.23] in Eq. [2.22] to simplify the Hamiltonian in Eq. [2.21],

$$\hat{H} = \hat{H}_e - \frac{e\lambda}{m}\sum_j(\hat{\mathbf{p}}_j\cdot\vec{\boldsymbol{\epsilon}})\hat{q} + \frac{\omega\lambda^2 e^2 N_e}{m}\hat{q}^2\,, \tag{2.24}$$

where $\hat{H}_e = \sum_j \frac{\hat{p_j}^2}{2m} + \hat{V}_{ee} + \hat{V}_{en} + V_{nn}$ is the electronic Hamiltonian and $\hat{q}_\alpha = \frac{1}{\sqrt{2\omega}}(\hat{b}^\dagger + \hat{b})$ is the photon canonical position operator. Lastly, we will transform the Hamiltonian into length gauge using the unitary transformation

$$\hat{U} = \exp\left[i\lambda e\sum_j(\hat{\mathbf{r}}_j\cdot\epsilon)\hat{q}\right]. \tag{2.25}$$

After some algebraic manipulation we get our final Hamiltonian[40],

$$\hat{H} = \hat{H}_e + \frac{1}{2}\left[\hat{p}^2 + \omega^2\left(\hat{q} + \frac{\lambda}{\omega}(\vec{\boldsymbol{\epsilon}}\cdot\hat{\mathbf{d}})\right)^2\right]. \tag{2.26}$$

Here $\hat{p} = i\sqrt{\frac{\omega}{2}}(\hat{b}^\dagger - \hat{b})$ is the canonical momentum operator and $\hat{\mathbf{d}}$ is the dipole operator,

$$\hat{\mathbf{d}} = \sum_i Z_i\hat{\mathbf{r}}_i, \tag{2.27}$$

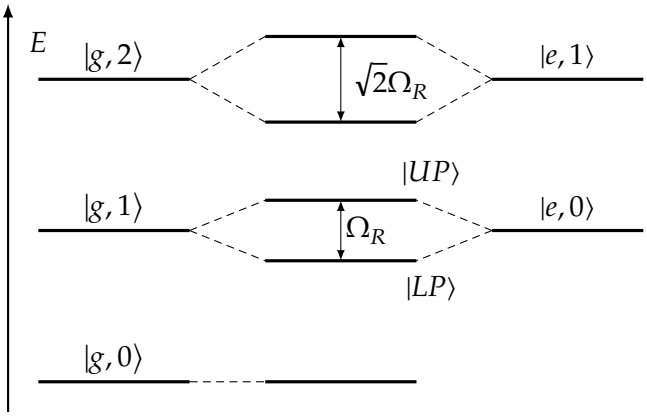

Figure 2.2 / Diagram showing the coupling of a two-state system $|g\rangle$ and $|e\rangle$ coupling with a resonant cavity with n photons, $|n\rangle$. The energy difference of the upper polariton (UP) and lower polariton (LP) is given in terms of the Rabi splitting Ω_R.

where $\hat{\mathbf{r}}_i$ and Z_i is the position operator and charge of the i-th particle.

2.3 Cavity QED

Cavity QED is the study of the light-matter interaction inside optical cavities. Within a cavity, the quantized field is coupled to the molecule creating light-matter states. The geometry and quality of the optical cavity may be modified to change which photon modes are present within the cavity, and how strong the light-matter coupling is. The combined light-matter states are known as *polaritons*, and in the simplest case they are a superposition of the system with zero and one photon, see Figure 2.2. The polaritons split into two states, where the lower energy state is called a lower polariton, and the higher energy state is called the upper polariton. The energy difference between the lower and upper polariton is the Rabi splitting Ω_R,

$$\Omega_R = \sqrt{\frac{2\omega}{\epsilon_0 V}} \left\| \vec{\mathbf{d}}_{fi} \right\| . \qquad [2.28]$$

The Rabi splitting is commonly used to demonstrate light-matter coupling, and will be used to quantify the coupling regime after we have introduced the decay rates in cavities.

2.3.1 Optical Cavities

An optical cavity is a set of highly reflective mirrors where light is reflected back and forth several times before dissipating. Interference between the waves creates quantized standing waves with frequency determined by the cavity geometry. The

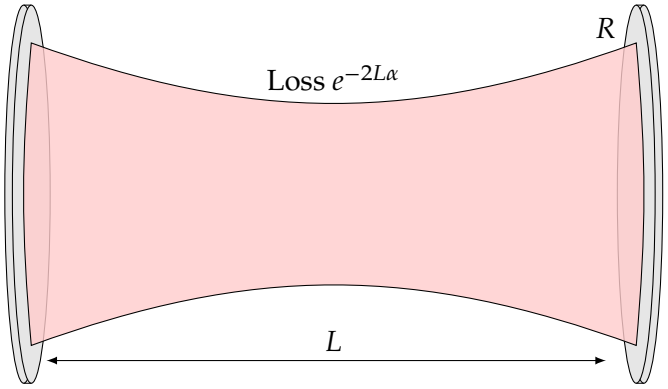

Figure 2.3 / A Fabry-Pérot resonator with reflectivity R, distance L and loss due to internal absorption and scattering $e^{-2L\alpha}$.

simplest cavity is a linear cavity, where two mirrors are placed at distance L apart from each other such that light continuously bounced back and forth[41]. An example of this is the Fabry-Pérot resonator, see Figure 2.3. Consider a photon inside this cavity. Each round trip is only partially reflected,

$$E(t) = R^N E(0)\,, \tag{2.29}$$

where E is the energy, N is the number of round trips, and R is the reflectivity of the mirrors. The number of round trips per time depends on the distance between the mirrors, $N = ct/2L$,

$$E(t) = E(0)e^{-\frac{1}{2}\kappa t}\,, \tag{2.30}$$

where $\kappa = -c\ln(R)/L$ is the decay rate. More generally we can also lose photons due to internal absorption and scattering, which replaces the decay rate κ with

$$\kappa = \frac{c(2L\alpha - \ln R)}{L}\,, \tag{2.31}$$

where α is the loss coefficient[41]. The stability of the cavity is given by the quality factor, $Q = \omega/\kappa$, which in this case is

$$Q = \frac{2\omega L}{c(2L\alpha - \ln(R))} \approx \frac{2\omega L}{c(2L\alpha + 1 - R)}\,. \tag{2.32}$$

The lifetime of a photon inside a cavity is the inverse of the decay rate,

$$\tau = \kappa^{-1} = \frac{L}{c(2L\alpha - \ln R)}\,. \tag{2.33}$$

Quantifying whether we are in the strong or ultra-strong coupling depends on how large the coupling strength λ, decay rate κ, and molecular emission Γ. Strong coupling

refers to when the lifetime of the cavity is long enough so that the system can emit and reabsorb photons multiple times. In other words, when the Rabi splitting Ω_R is large,

$$\Omega_R \gg (\kappa, \Gamma)\,, \tag{2.34}$$

then we are in the strong coupling regime[35, 42].

2.3.2 Two-Level Models

Consider the light-matter Hamiltonian Eq. [2.26] in terms of photon annihilation and creation operators,

$$\hat{H} = \hat{H}_e + \omega_{cav}\hat{b}^\dagger\hat{b} + \alpha\hat{d}(\hat{b}^\dagger + \hat{b}) + \beta\hat{d}^2\,, \tag{2.35}$$

where we have introduced

$$\alpha = \lambda\sqrt{\frac{\omega_{cav}}{2}}, \quad \beta = \frac{\lambda^2}{2}\,. \tag{2.36}$$

Assume now that we have a two-level electronic system with states $|g\rangle$ and $|e\rangle$ with energies E_g and E_e respectively. In this case we can simplify the Hamiltonian. First consider the electronic Hamiltonian $\hat{H}_e$,

$$\hat{H}_e = \frac{1}{2}(E_g + E_e) - \frac{1}{2}\omega_{eg}\hat{\sigma}_z\,, \tag{2.37}$$

where $\omega_{eg} = E_e - E_g$ is the electronic excitation energy and $\hat{\sigma}$ is the Pauli spin matrix. $\frac{1}{2}(E_g + E_e)$ corresponds only to a constant shift in the Hamiltonian in energy. We set $E_g = -E_e$ without loss of generality. Similarly, we may write the dipole operator in the two-state basis as

$$\hat{d} = \frac{1}{2}(d_{gg} + d_{ee}) - \frac{1}{2}(d_{ee} - d_{gg})\hat{\sigma}_z + d_{eg}\hat{\sigma}_x\,. \tag{2.38}$$

The Hamiltonian is translation invariant as shown in Section 4.1.1, meaning that we can choose a geometry where $d_{ee} = -d_{gg}$. The two-state Hamiltonian [2.35] may be written as

$$\hat{H} = \frac{1}{2}\omega_{cav}\hat{b}^\dagger\hat{b} - \frac{1}{2}\omega_{eg}\hat{\sigma}_z + \alpha(d_{eg}\hat{\sigma}_x - \frac{1}{2}\delta\hat{\sigma}_z)(\hat{b}^\dagger + \hat{b}) + \beta(\delta^2 + d_{eg}^2)\,, \tag{2.39}$$

where $\delta = d_{ee} - d_{gg}$ is the change in dipole between the states. The dipole self-energy is just a constant shift in the energy in the two-state scenario. This is not valid for more than two-states, where the self-energy will change the dynamics of the system. The Hamiltonian of Eq. [2.39] corresponds to the extended Rabi model studied in circuit QED[43]. Assuming that the change in dipole is zero, $\delta = 0$, brings us to the standard Rabi model with a self-energy term. The full spectrum of the Rabi model has been found[44], but it cannot be written in terms of simple equations.

The simplest model with an analytical solution to describe interactions between a molecule and the electromagnetic field is the Jaynes-Cummings model (JCM)[17],

$$\hat{H} = \omega_{cav}\hat{b}^\dagger\hat{b} - \frac{1}{2}\omega_{eg}\hat{\sigma}_z + \frac{1}{2}\Omega_R(\hat{b}^\dagger |g\rangle\langle e| + \hat{b}\,|e\rangle\langle g|)\,, \qquad [2.40]$$

where $\Omega_R = 2\lambda d_{eg}\sqrt{\frac{2}{\omega}}$ is the coupling parameter known as the Rabi splitting. The Jaynes-Cummings model is recovered from the two-state system Eq. [2.39] by the rotating wave approximation (RWA) and setting $\delta = 0$.

Here we will show how the JCM is diagonalized. Based on the interaction term in Eq. [2.40], we choose an orthonormal basis $\{|g,0\rangle, |e,0\rangle, |g,n\rangle, |e,n\rangle, \dots\}$ where $|n\rangle$ is the photon number state. The Hamiltonian in this basis is nearly diagonal,

$$\mathbf{H} = \begin{bmatrix} 0 & & & \\ & [H_0] & & \\ & & [H_1] & \\ & & & \ddots \end{bmatrix} - \frac{1}{2}\omega_{eg}\mathbf{I}\,. \qquad [2.41]$$

$[H_n]$ is the Hamiltonian in the reduced basis $\{|e,n\rangle, |g,n+1\rangle\}$,

$$[H_n] = \begin{bmatrix} n\omega_{cav} + \omega_{eg} & \Omega_R\sqrt{n+1} \\ \Omega_R\sqrt{n+1} & (n+1)\omega_{cav} \end{bmatrix}, \qquad [2.42]$$

$$= (n\omega_{cav} + \omega_{eg})\mathbf{I} + \begin{bmatrix} 0 & \Omega_R\sqrt{n+1} \\ \Omega_R\sqrt{n+1} & \Delta\omega \end{bmatrix}, \qquad [2.43]$$

where $\Delta\omega = \omega_{cav} - \omega_{eg}$. Since the non-diagonal elements are zero, there's no interaction between the different reduced Hamiltonians. The energies and states are therefore independent. Instead of looking at the Hamiltonian in the full basis, we may solve the Hamiltonian in the reduced basis. Diagonalizing Eq. [2.42] gives the energy,

$$E_{\pm,n} = \omega_{eg} + n\omega_{cav} + \frac{1}{2}\Delta\omega \pm \frac{1}{2}\sqrt{(\Delta\omega)^2 + 4\Omega_R^2(n+1)}\,. \qquad [2.44]$$

The eigenstates of the reduced Hamiltonian, known as *dressed states*, are

$$|\psi_{\pm,n}\rangle = \begin{bmatrix} \frac{\Delta\omega \pm \sqrt{(\Delta\omega)^2 + 4\Omega_R^2(n+1)}}{2\Omega_R\sqrt{n+1}} \\ -1 \end{bmatrix}. \qquad [2.45]$$

The eigenstate can be immensely simplified by defining a new variable θ_n,

$$\tan(\theta_n) = \frac{\Delta\omega + \sqrt{(\Delta\omega)^2 + 4\Omega_R^2(n+1)}}{2\Omega_R\sqrt{n+1}}. \quad [2.46]$$

Inserting Eq. [2.46] into [2.45], we find one of the eigenstates,

$$|\psi_{+,n}\rangle = \begin{bmatrix} \cos(\theta_n) \\ -\sin(\theta_n) \end{bmatrix}. \quad [2.47]$$

From Eq. [2.44], for a non-zero interaction the energies of the states are different. Therefore the eigenstates must be orthogonal and is found to be

$$|\psi_{-,n}\rangle = \begin{bmatrix} \sin(\theta_n) \\ \cos(\theta_n) \end{bmatrix}. \quad [2.48]$$

The diagonalized Hamiltonian is

$$[H_n] = \begin{bmatrix} \cos(\theta_n) & \sin(\theta_n) \\ -\sin(\theta_n) & \cos(\theta_n) \end{bmatrix}^{-1} \begin{bmatrix} E_+ & 0 \\ 0 & E_- \end{bmatrix} \begin{bmatrix} \cos(\theta_n) & \sin(\theta_n) \\ -\sin(\theta_n) & \cos(\theta_n) \end{bmatrix} \quad [2.49]$$

$$= \mathbf{R}(-\theta_n) \begin{bmatrix} E_+ & 0 \\ 0 & E_- \end{bmatrix} \mathbf{R}(\theta_n), \quad [2.50]$$

where $\mathbf{R}(\theta)$ is the clockwise rotation matrix. The eigenstates of JCM, the dressed states, are a rotation of states $\{|e,n\rangle, |g,n+1\rangle\}$ as illustrated in Figure 2.4.

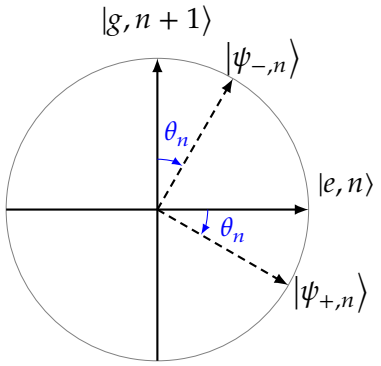

Figure 2.4 / Dressed states $\{|\psi_{\pm,n}\rangle\}$ are created from rotations in the $\{|e,n\rangle, |g,n+1\rangle\}$ basis.

Note that even for the vacuum state $n = 0$, θ_n is non-zero. This entails that the photon vacuum state is creating an interaction with the molecule. This effect can be measured from the difference in energy Eq. [2.44]. The JCM ground state with zero photons is

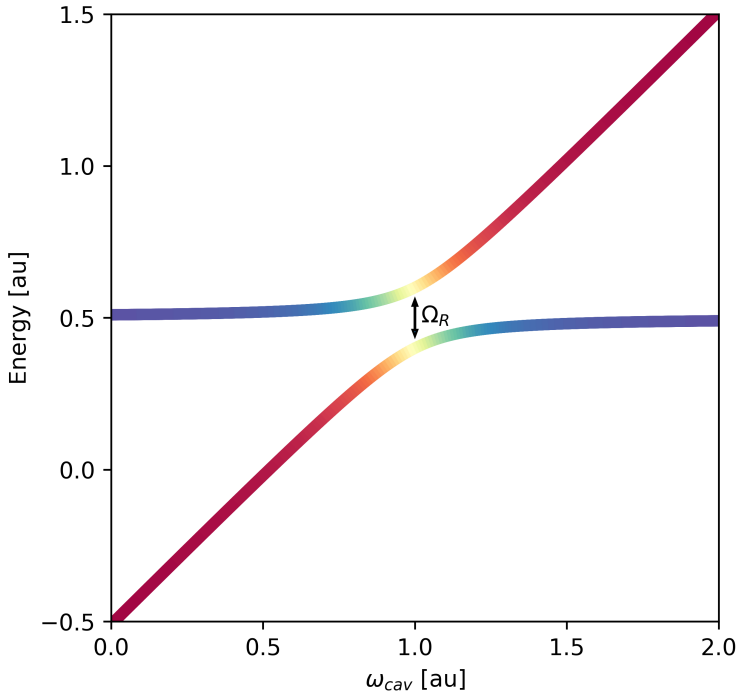

Figure 2.5 / Interaction between an excited state and the ground state photon line for JCM with coupling $\Omega_R = 0.20$. Red is $|g,1\rangle$, blue is $|e,0\rangle$, and the polariton is yellow.

not interacting with any other state Eq. [2.41], and the energy remains unchanged. In Figure 2.5 the states for $n = 0$ has been visualized. The blue horizontal lines corresponds to electronic states, $|g,0\rangle$ and $|e,0\rangle$. The red diagonal lines coming from the ground state and excited states are known as photon lines, and corresponds to states of the form $|g,n\rangle$ and $|e,n\rangle$ for $n \geq 1$. The most important case of JCM is when the photons are in resonance with the two-state system, $\Delta\omega \approx 0$, where the dressed states are known as *polaritons*. This corresponds to where the the light-matter interaction is the greatest as seen from Eq. [2.46]. The polaritons are illustrated as the curved yellow states in Figure 2.5.

Rest of this page intentionally left blank.

Chapter 3

Fundamentals of Coupled Cluster Theory

Electronic structure theory is a field dedicated to solve the Schrödinger equation,

$$\hat{H}\,|\Psi\rangle = E\,|\Psi\rangle\,, \tag{3.1}$$

for the electronic systems. In this thesis, we will limit ourselves to closed shell molecules in the Born-Oppenheimer approximation, where nuclei are stationary. We will be using atomic units. General orbitals will be indexed m, n, p, q, r, s, occupied as i, j, k, l and virtual as a, b, c, d.

The electronic Hamiltonian in second quantization can be written

$$\hat{H}_e = \sum_{pq} h_{pq} E_{pq} + \sum_{pqrs} g_{pqrs} e_{pqrs} + h_{\text{nuc}} \tag{3.2}$$

Here E_{pq} is the one electron singlet excitation operator and e_{pqrs} is the two-electron singlet excitation operator,

$$E_{pq} = \sum_{\sigma} \hat{a}^{\dagger}_{p\sigma} \hat{a}_{q\sigma} \tag{3.3}$$

$$e_{pqrs} = \sum_{\sigma_1 \sigma_2} \hat{a}^{\dagger}_{p\sigma_1} \hat{a}^{\dagger}_{r\sigma_2} \hat{a}_{s\sigma_2} \hat{a}_{q\sigma_1} \tag{3.4}$$

where $\hat{a}/\hat{a}^{\dagger}$ is the electron creation operator and σ is the spin of the electron. The zero-, one- and two-electron integrals h_{nuc}, h_{pq} and g_{pqrs} are defined from the operators

$$h_{\text{nuc}} = \frac{1}{2} \sum_{I \neq J}^{\text{nuclei}} \frac{Z_I Z_J}{|R_I - R_J|} \tag{3.5}$$

$$\hat{h}(i) = -\frac{1}{2}\hat{\nabla}_i^2 - \sum_{I}^{\text{nuclei}} \frac{Z_I}{|\hat{r}_i - R_I|} \tag{3.6}$$

$$\hat{g}(i,j) = \frac{1}{|\hat{r}_i - \hat{r}_j|} \tag{3.7}$$

where Z_I and R_I are the I-th nuclear charge and position, and $\hat{r}_i$ is the i-th electron position operator.

The electrons are fermions, which are anti-symmetric. In first quantization, this anti-symmetry is described by the wavefunctions. For non-interacting particles we have the Slater determinant. In second quantization, anti-symmetry is moved from the wavefunction to the operators, giving rise to the anti-commutation relations,

$$[\hat{a}_{p\sigma}, \hat{a}_{q\tau}]_+ = 0 \quad [3.8]$$
$$[\hat{a}^\dagger_{p\sigma}, \hat{a}^\dagger_{q\tau}]_+ = 0 \quad [3.9]$$
$$[\hat{a}_{p\sigma}, \hat{a}^\dagger_{q\tau}]_+ = \delta_{p\sigma,q\tau} \quad [3.10]$$

Using the commutation relations Eqs. (3.8-3.10) the singlet excitation commutators can be derived,

$$[E_{pq}, E_{rs}] = E_{ps}\delta_{rq} - E_{rq}\delta_{ps} \quad [3.11]$$
$$[e_{pqrs}, E_{mn}] = \delta_{mq}e_{pnrs} - \delta_{pn}e_{mqrs} + \delta_{ms}e_{pqrn} - \delta_{rn}e_{pqms} \quad [3.12]$$

A similarity transformation of an operator does not change the eigenvalues. For the Hamiltonian and its eigenvalue, the energy, consider the Schrödinger equation using $|\Psi'\rangle = U|\Psi\rangle$,

$$H|\Psi'\rangle = E|\Psi'\rangle \Leftrightarrow U^{-1}HU|\Psi\rangle = E|\Psi\rangle\,. \quad [3.13]$$

This relation is used both to derive the Hartree-Fock and Coupled-Cluster equations. For further reading about electronic structure theory, Helgaker *et al.*'s book[23] is recommended.

3.1 Hartree-Fock Method

In this section we will give a brief introduction to the Hartree-Fock method in second quantization. Consider a closed shell N_e-electron state R,

$$|R\rangle = \left(\prod_i^{\frac{1}{2}N_e} \hat{a}^\dagger_{i\alpha}a^\dagger_{i\beta}\right)|vac\rangle\,. \quad [3.14]$$

The exact electronic wavefunction for the ground state would be described by a linear combination of all the different electron configurations of a molecule,

$$|GS\rangle = (C_0 + \sum_\mu C_\mu \hat{\tau}_\mu)\,|R\rangle \quad [3.15]$$

where $\hat{\tau}_\mu$ generates other configurations $|\mu\rangle$ from $|R\rangle$. The *Hartree-Fock method* (HF) assumes that a single state $|R\rangle$ can describe all the interactions, effectively setting $C_\mu = 0$

in Eq. [3.15]. Using the variational principle on $|R\rangle$ we find the molecular orbitals (MO) that minimizes the energy. This is the ground state in the HF method. The difference in energy from $|R\rangle$ to the exact wavefunction is known as the *correlation energy* and is a result of the two-electron terms causing electron-electron correlation. In this thesis we will use restricted HF, limiting us to closed-shell molecules.

Transforming a set of orthonormal MO to a new set of orthonormal MO is known as orbital rotation. We will use the anti-Hermitian operator $\hat{\kappa}$ to generate rotations,

$$|R(\kappa)\rangle = e^{\hat{\kappa}} |R\rangle \tag{3.16}$$

where $\hat{\kappa}$ is

$$\hat{\kappa} = \sum_{p>q} \kappa_{pq}(E_{pq} - E_{qp}). \tag{3.17}$$

Rotations between occupied-occupied can be shown to be zero by using $i \neq j$ and the commutation relations,

$$E_{ij}|R\rangle = E_{ij} \prod_k a^\dagger_{k\alpha} a^\dagger_{k\beta} |vac\rangle \tag{3.18}$$

$$= \left(\prod_k a^\dagger_{k\alpha} a^\dagger_{k\beta} \right) E_{ij} |vac\rangle + [E_{ij}, \prod_k a^\dagger_{k\alpha} a^\dagger_{k\beta}] |vac\rangle \tag{3.19}$$

$$= 0 \tag{3.20}$$

A similar argument follows for virtual-virtual rotations. Therefore we only need to account for rotations between occupied and virtual MO,

$$\hat{\kappa} = \sum_{ai} \kappa_{ai}(E_{ai} - E_{ia}). \tag{3.21}$$

The energy is given as a Baker-Campbell-Hausdorff (BCH) expansion of the exponential,

$$E(\kappa) = \langle R(\kappa)|H|R(\kappa)\rangle = \langle R|H + [H, \hat{\kappa}] + \frac{1}{2}[[H, \hat{\kappa}], \hat{\kappa}] + ...|R\rangle \tag{3.22}$$

The energy is in a stationary point when the derivative with respect to κ_{ai} is zero, which we will assume is a minimum. For an already minimized state $\kappa = 0$, which is the HF state,

$$\frac{\partial E(0)}{\partial \kappa_{ai}} = \langle HF|[H, E_{ai} - E_{ia}]|HF\rangle . \tag{3.23}$$

Assuming that the wavefunction is real, this expression may be simplified further,

$$\frac{\partial E(0)}{\partial \kappa_{ai}} = \langle HF|[H, E_{ai}]|HF\rangle + \langle HF|[H, E_{ai}]|HF\rangle^* , \tag{3.24}$$

$$= 2 \langle HF|[H, E_{ai}]|HF\rangle . \tag{3.25}$$

Equation [3.25] is recognized as the Brillouin Theorem[23],

$$\langle HF|\hat{H}|_i^a\rangle = 0. \tag{3.26}$$

The HF state does not interact with singly excited states. In the following section about Coupled-Cluster theory, this is used to simplify expressions. This is also the condition which is used to optimize Hartree-Fock by using the Fock matrix[23],

$$F_{pq} = -\frac{1}{2}\sum_{\sigma} \langle R|[[\hat{H}, \hat{a}_{p\sigma}], \hat{a}^{\dagger}_{q\sigma}]_+|R\rangle \ . \tag{3.27}$$

The MO that diagonalize the Fock matrix also satisfies the Brillouin Theorem [3.26], and consequently they are the optimized Hartree-Fock orbitals. It is important to emphasize that the Fock matrix is dependent on the MO. Diagonalizing the Fock matrix once does not give the correct state. The Fock matrix is instead solved as a self-consistent field (SCF), iteratively diagonalizing the matrix until the Fock matrix is self-consistent. A self-consistent diagonal Fock matrix is known as a *canonical* Fock matrix,

$$F_{pq} = \epsilon_p \delta_{pq} \tag{3.28}$$

where ϵ is the orbital energy. From the definition of the Fock matrix [3.27] on the electronic Hamiltonian [3.2], we get the well-known Fock matrix,

$$F_{pq} = h_{pq} + \sum_i \left(2g_{pqii} - g_{piiq}\right). \tag{3.29}$$

3.2 Coupled Cluster

Coupled cluster (CC) is a post-HF method, which improves upon the HF wavefunction by including electron-electron correlation. This is done by the excitation operators $\hat{T}$,

$$\hat{T} = \sum_{\mu} t_\mu \hat{\tau}_\mu \tag{3.30}$$

where $\hat{\tau}_\mu$ generates the excitation μ, and t_μ are coefficient known as the CC amplitudes. The wavefunction in CC uses an exponential ansatz,

$$|CC\rangle = e^{\hat{T}}|HF\rangle \, . \tag{3.31}$$

The excitation operator is split into levels of excitation,

$$\begin{aligned} \hat{T} &= \hat{T}_1 + \hat{T}_2 + \cdots + \hat{T}_{N_e} \\ &= \sum_{\mu_1} t_{\mu_1}\hat{\tau}_{\mu_1} + \sum_{\mu_2} t_{\mu_2}\hat{\tau}_{\mu_2} + \ldots \end{aligned} \tag{3.32}$$

where $\hat{T}_1$ generates single excitations, $\hat{T}_2$ generates double excitations and $\hat{T}_{N_e}$ excites all the electrons in the system. The amplitudes in Eq. [3.30] are determined by projection instead of variationally, due to the variational procedure being very computationally expensive[23]. Starting from Schrödinger's equation [3.1],

$$\hat{H}e^{\hat{T}}\left|HF\right\rangle = Ee^{\hat{T}}\left|HF\right\rangle, \tag{3.33}$$

we remove the exponential from the right side,

$$e^{-\hat{T}}\hat{H}e^{\hat{T}}\left|HF\right\rangle = E\left|HF\right\rangle. \tag{3.34}$$

This is the *CC similarity transformed* Hamiltonian,

$$\hat{H}^T = e^{-\hat{T}}\hat{H}e^{\hat{T}}. \tag{3.35}$$

3.2.1 Ground State

Whereas the HF ground state is found by minimizing the energy, the CC ground state is determined from the *projection equation*, which determines the CC amplitudes. The projection equation is the similarity transformed Hamiltonian Eq. 3.34 projected onto an excited state $\langle\overline{\mu}|$, which for the optimized CC state should be

$$\langle\overline{\mu}|\hat{H}^T|HF\rangle = 0. \tag{3.36}$$

The overline means normalized with respect to $\langle\overline{\mu}|\hat{\tau}_\mu|HF\rangle = 1$. Only for the optimized CC amplitudes are the projection equations [3.36] fulfilled. We define Ω_μ

$$\Omega_\mu = \langle\overline{\mu}|\hat{H}^T|HF\rangle, \tag{3.37}$$

which in general is not zero. By expanding the similarity transformed Hamiltonian using the BCH expansion, an explicit equation for Ω_μ is obtained. The CC ground state is determined by choosing amplitudes which minimize Ω_μ in an iterative scheme. When the amplitudes are determined, the energy can be calculated from

$$E_{\mathrm{CC}} = E_{\mathrm{HF}} + \sum_{aibj}(t_{ij}^{ab} + t_i^a t_j^b)\left(2g_{iajb} - g_{ibja}\right). \tag{3.38}$$

The energy only has contributions from the singles and doubles amplitudes. However, adding triples and higher excitations will change the singles and doubles amplitudes via the projection equation Eq. [3.36], indirectly changing the energy.

3.2.2 Excited states

One important part of electronic structure theory is the calculations of properties. There are two widely recognized methods within CC to compute properties. One is

linear response[45, 46], and the other is equation-of-motion CC(EOM-CC)[47]. For the excitation energies, the methods are equivalent[45]. Here we will briefly introduce how excitation energies are calculated in CC.

Consider the similarity transformed Hamiltonian matrix in a basis $\{|R\rangle, |\mu\rangle\}$, where μ includes all single excitations for CCS, single and doubles for CCSD etc.

$$\mathbf{H}^T = \begin{bmatrix} E_0 & \vec{\boldsymbol{\eta}} \\ \vec{\boldsymbol{\Omega}} & \mathbf{A} + E_0\mathbf{I} \end{bmatrix}. \tag{3.39}$$

Here $\mathbf{I}$ is the identity matrix, $\mathbf{A}$ is the *CC Jacobian matrix*,

$$A_{\mu\nu} = \langle \overline{\mu}|\hat{H}^T|\nu\rangle - E_0\delta_{\mu\nu} = \langle \overline{\mu}|[\hat{H}^T, \hat{\tau}_\nu]t|R\rangle \ , \tag{3.40}$$

and $\vec{\boldsymbol{\eta}}$ is

$$\eta_\nu = \langle HF|\hat{H}^T|\nu\rangle \ . \tag{3.41}$$

In the optimized CC ground state, the projection equations [3.36] are fulfilled,

$$\mathbf{H}^T = \begin{bmatrix} E_0 & \vec{\boldsymbol{\eta}} \\ 0 & \mathbf{A} + E_0\mathbf{I} \end{bmatrix}. \tag{3.42}$$

Since the lower left block of $\mathbf{H}^T$ is zero, the eigenvalues of $\mathbf{H}^T$ are independent of $\vec{\boldsymbol{\eta}}$. In other words, there is no contribution in energy in the interaction between the ground state and excited states. Determining the excited state energies is the same as finding the eigenvalues of the Jacobian, Eq. [3.40], and adding the ground state energy. Or equivalently, the eigenvalues of the Jacobian corresponds to excitation energies. It is important for later discussion to know that this is true only if the projection equations [3.36] are fulfilled. If $\vec{\boldsymbol{\Omega}} \neq 0$, then the eigenvalues of the Jacobian are no longer the excitation energies.

Chapter 4

QED-CC

4.1 Hamiltonian

The light-matter Hamiltonian that was derived from the Pauli-Fierz Hamiltonian[39] in Section 2.2.1 will be used in QED-CC. Three approximations were used in the derivation,

- Born-Oppenheimer Approximation,
- Dipole Approximation,
- Single-Mode Approximation.

The Hamiltonian in the Coulomb and length gauge can be written in terms of photon creation and annihilation operators $\hat{b}^\dagger$ and $\hat{b}$,

$$\hat{H} = \hat{H}_e + \omega \hat{b}^\dagger \hat{b} + \alpha \hat{d}(\hat{b}^\dagger + \hat{b}) + \beta \hat{d}^2 \,. \tag{4.1}$$

Here $\hat{H}_e$ is the electronic Hamiltonian and ω is the photon frequency and $\hat{d}$ is the dipole dotted with the transversal polarization vector of the photons $\vec{\epsilon}$,

$$\hat{d} = \sum_{pq} (\vec{\boldsymbol{\epsilon}} \cdot \vec{\mathbf{d}}_{pq}) E_{pq} = \sum_{pq} d_{pq} E_{pq} \,. \tag{4.2}$$

The matrix d_{pq} was introduced as $\vec{\boldsymbol{\epsilon}} \cdot \vec{\mathbf{d}}_{pq}$ for convenience, and includes both the electrons and the nuclei in the dipole. The coefficients α and β are defined as

$$\alpha = \lambda \sqrt{\frac{\omega}{2}}, \quad \beta = \frac{\lambda^2}{2}, \tag{4.3}$$

where $\lambda = \frac{4\pi}{V}$ is the coupling strength.

The third term in Eq. [4.1], the *bilinear coupling*, couples the dipole to the photons which allows the molecule to annihilate and create photons. The bilinear coupling is what generates the change in the electromagnetic field. If a molecule has a weak dipole, the changes in the field are likely to be small. The fourth term of Eq. [4.1] is

the *dipole self-energy*, and will be present for all atoms and molecules in cavities. This is because every system of charged particles has a fluctuation of the dipole moment from the uncertainty principle. The dipole self-energy is sometimes ignored since it corresponds to a constant shift in energy in the Jaynes-Cummings and Rabi model. Rokaj *et al.* have shown that for proper light-matter systems there exists no ground state when ignoring the dipole self-energy[48]. To be physically accurate, the dipole self-energy must be included.

4.1.1 Translation Invariance

The dipole of a molecule is defined as

$$\hat{\mathbf{d}} = \sum_i Z_i \vec{r}_i \,, \tag{4.4}$$

where Z_i is the charge and r_i is the position of the i-th particle. For a non-charged system the dipole will stay the same when we move the origin,

$$\hat{\mathbf{d}} = \sum_i Z_i(\vec{\mathbf{r}}_i + \Delta\vec{\mathbf{r}}) = \sum_i Z_i \vec{\mathbf{r}}_i + \Delta\vec{\mathbf{r}} \sum_i Z_i = \sum_i Z_i \vec{\mathbf{r}}_i \,. \tag{4.5}$$

This is known as *translation invariance*. For a charged molecule, this invariance is lost. We now want to investigate the translational invariance for our Hamiltonian. A shift in the dipole is introduced into Eq. [2.26],

$$\hat{H} = \hat{H}_e + \frac{1}{2}\left[\hat{p}^2 + \omega^2\left(\hat{q} + \frac{\lambda}{\omega}\hat{d} + \frac{\lambda}{\omega}\Delta d\right)^2\right], \tag{4.6}$$

here written in terms of the canonical position and momentum $\hat{q}$ and $\hat{p}$ respectively. The displacement operator $\hat{D}$ is

$$\hat{D}(q_0) = e^{iq_0\hat{p}} \,, \tag{4.7}$$

and can be used to easily displace $\hat{q}$ via a similarity transformation,

$$\hat{D}(q_0)^\dagger \hat{q} \hat{D}(q_0) = \hat{q} + q_0 \,. \tag{4.8}$$

Similarity transformations do not change the energy. We may remove the shift in dipole by transforming the Hamiltonian with the displacement operator [4.7] and choosing $q_0 = -\frac{\lambda}{\omega}\Delta d$,

$$\begin{aligned} \hat{D}(q_0)^\dagger \hat{H} \hat{D}(q_0) &= \hat{H}_e + \frac{1}{2}\left[\hat{p}^2 + \omega^2\left(\hat{q} + q_0 + \frac{\lambda}{\omega}\hat{d} + \frac{\lambda}{\omega}\Delta d\right)^2\right], \\ &= \hat{H}_e + \frac{1}{2}\left[\hat{p}^2 + \omega^2\left(\hat{q} + \frac{\lambda}{\omega}\hat{d}\right)^2\right]. \end{aligned} \tag{4.9}$$

Thus the translation invariance of the system is recovered by the photons, even for charged molecules with origin dependent dipoles.

4.1.2 Coherent State Basis

The displacement operator [4.7] is equivalent to the operator producing coherent states[36] for a real parameter z,

$$|z\rangle = e^{z(\hat{b}^\dagger - \hat{b})}\,|0\rangle = \hat{D}\left(z \cdot \sqrt{\frac{2}{\omega}}\right)|0\rangle\ . \tag{4.10}$$

Hence, the translation invariance of the Hamiltonian is closely related to coherent states, as seen in Eq. [4.10]. In light of this, *generalized coherent states*[37, 38] will be used for the photon basis instead of the standard photon number states. The generalized coherent states are defined as

$$|z, n\rangle = e^{z\hat{b}^\dagger - z^*\hat{b}}\,|n\rangle\ , \tag{4.11}$$

where z is in general a complex parameter, but we will only consider the scenario where z is real, $z = z^*$. The Schrödinger equation with generalized coherent states is

$$\hat{H}\,|z, n\rangle = E\,|z, n\rangle\ , \tag{4.12}$$

or equivalently in terms of a similarity transformation,

$$\hat{H}'\,|n\rangle = e^{-z(\hat{b}^\dagger - \hat{b})}\hat{H}e^{z(\hat{b}^\dagger - \hat{b})}\,|n\rangle = E\,|n\rangle\ . \tag{4.13}$$

The similarity transformed Hamiltonian $\hat{H}'$ may be simplified by using the BCH expansion,

$$\hat{H}' = \hat{H}_e + \beta\hat{d}^2 + \alpha\hat{d}(\hat{b}^\dagger + \hat{b} + 2z) + \omega(\hat{b}^\dagger + z)(\hat{b} + z)\,. \tag{4.14}$$

Taking the average over the electronic state $|R\rangle$,

$$\langle R|\hat{H}'|R\rangle = E_0 + (\hat{b}^\dagger + \hat{b})(\alpha\,\langle d\rangle_R + \omega z) + \omega\hat{b}^\dagger\hat{b}\,, \tag{4.15}$$

where $E_0 = \langle H_e\rangle_R + \omega z^2 + 2\alpha\,\langle d\rangle_R\, z + \beta\left\langle d^2\right\rangle_R$ is a constant. Choosing

$$z = -\frac{\alpha\,\langle d\rangle}{\omega}\,, \tag{4.16}$$

diagonalizes Eq. [4.15]. Inserting Eq. [4.16] into Eq. [4.14] gives the final expression for the Hamiltonian in the coherent state basis,

$$\hat{H}' = \hat{H}_e + \alpha(\hat{d} - \langle d\rangle_R)(\hat{b}^\dagger + \hat{b}) + \beta(\hat{d} - \langle d\rangle_R)^2 + \omega\hat{b}^\dagger\hat{b}\,. \tag{4.17}$$

In this Hamiltonian the excitations of photons are dependent on fluctuations from the dipole away from the mean-field dipole. If the reference state is chosen to be the ground state, the Hamiltonian is formulated in terms of changes relative to the ground state dipole. The ground state dipole self-energy in this basis is simply the variance of the dipole moment. This is the Hamiltonian that will be used in the QED Hartree-Fock and QED Coupled-Cluster methods.

4.1.3 Photon Ordering

The Hamiltonian in Eq. [4.17] is not ideal for deriving the CC equations. Doing a similarity transformation with only 1 photon coupled to the electronic single excitations adds over 10 new terms. In this section the Hamiltonian will rewritten such that it easily extends to many photons.

Firstly, the Hamiltonian [4.17] can be sorted in orders of $\hat{b}^\dagger$,

$$\hat{H} = \left(\hat{H}_e + \beta(\hat{d} - \langle d \rangle_R)^2\right) + \left(\alpha(\hat{d} - \langle d \rangle_R)\right)\hat{b}^\dagger + \left(\alpha(\hat{d} - \langle d \rangle_R)\right)\hat{b} + \omega\hat{b}^\dagger\hat{b}. \tag{4.18}$$

The two first terms of Eq. [4.18] can be rewritten in terms of one-electron, two-electron and constant terms,

$$\begin{aligned}\hat{H}_e + \beta(\hat{d} - \langle d \rangle)^2 = &\sum_{pq}\left(h_{pq} + \beta[d^2]_{pq} - 2\beta\langle d \rangle_R d_{pq}\right)E_{pq} \\ &+ \frac{1}{2}\sum_{pqrs}\left(g_{pqrs} + 2\beta d_{pq}d_{rs}\right)e_{pqrs} + \left(h_{\text{nuc}} + \beta\langle d \rangle_R^2\right).\end{aligned} \tag{4.19}$$

We define $\hat{H}_e^{(0)}$ and $c^{(0)}$ and new one- and two-electron integrals $h_{pq}^{(0)}$ and $g_{pqrs}^{(0)}$,

$$h_{pq}^{(0)} = h_{pq} + \beta[d^2]_{pq} - 2\beta\langle d \rangle_R d_{pq} \tag{4.20}$$

$$g_{pqrs}^{(0)} = g_{pqrs} + 2\beta d_{pq}d_{rs} \tag{4.21}$$

$$c^{(0)} = h_{\text{nuc}} + \beta\langle d \rangle_R^2 \tag{4.22}$$

$$\hat{H}_e^{(0)} = \sum_{pq} h_{pq}^{(0)}E_{pq} + \frac{1}{2}\sum_{pqrs} g_{pqrs}^{(0)}e_{pqrs} \tag{4.23}$$

Similarly, the terms which are first order in $\hat{b}^\dagger$ in the Hamiltonian [4.18] can be introduced in the one-electron integrals and a constant term,

$$h_{pq}^{(1)} = \alpha d_{pq} \tag{4.24}$$

$$g_{pqrs}^{(1)} = 0 \tag{4.25}$$

$$c^{(1)} = -\alpha\langle d \rangle_R \tag{4.26}$$

$$\hat{H}_e^{(1)} = \sum_{pq} h_{pq}^{(1)}E_{pq} + \frac{1}{2}\sum_{pqrs} g_{pqrs}^{(1)}e_{pqrs} \tag{4.27}$$

The Hamiltonian [4.18] may now be written in terms of the new integrals and constants,

$$\hat{H} = \sum_{n=0}^{1} \hat{b}^{\dagger n}\left(\hat{H}_e^{(n)} + c^{(n)}\right) + \alpha\left(\hat{d} - \langle d\rangle\right)\hat{b} + \omega\hat{b}^\dagger\hat{b} \qquad [4.28]$$

Finally, $\tilde{}$ is introduced as the sum over all the photon orders for a general operator $\hat{O}$,

$$\tilde{O} = \sum_{n=0} \hat{b}^{\dagger n}\hat{O}^{(n)}, \qquad [4.29]$$

where undefined terms are zero, for instance $\hat{H}_e^{(2)} = 0$. The final expression for the Hamiltonian is

$$\hat{H} = \tilde{H}_e + \tilde{c} + \alpha\left(\tilde{d} - \langle d\rangle_R\right)\hat{b} + \omega\hat{b}^\dagger\hat{b}. \qquad [4.30]$$

where $d_{pq}^{(0)} = d_{pq}$. This Hamiltonian is useful because, as we will show, transforming it using $e^{-\hat{T}_S}He^{\hat{T}_S}$ will only change the one- and two-electron integrals. The form of the Hamiltonian will remain the same.

$$\hat{T}_S = \hat{T}_1 + \sum_{n=1} \hat{S}_n\hat{b}^{\dagger n} + \sum_{m=1} \gamma_m\hat{b}^{\dagger m} \qquad [4.31]$$

Here $\hat{T}_1$ and $\hat{S}_n$ generates single excitations in the electronic wavefunction.

4.2 Exponential Ansatz

The Hamiltonian used for QED-CC is the coherent state transformed Hamiltonian Eq. [4.30]. We will in this section show the extension of the exponential ansatz to QED-CC. We will choose $\hat{b}^\dagger$ as the photon excitation operator. In terms of this excitation the exponential ansatz to QED-CC is

$$|CC\rangle = e^{\hat{T}}|R\rangle\,. \qquad [4.32]$$

Here $\hat{T}$ is the excitation operator

$$\hat{T} = \hat{T}_{el} + \sum_{n=1} \hat{T}_{el,n}\hat{b}^{\dagger n} + \sum_{n=1} \gamma_n\hat{b}^{\dagger n}, \qquad [4.33]$$

where γ_n are the amplitudes for the pure photon excitation and $\hat{T}_{el}$ and $\hat{T}_{el,n}$ are electronic excitation operator,

$$\begin{aligned}\hat{T}_{el} &= \hat{T}_1 + \hat{T}_2 + \ldots \\ &= \sum_{ai} t_{ai}E_{ai} + \sum_{aibj} t_{aibj}E_{ai}E_{bj} + \ldots,\end{aligned} \qquad [4.34]$$

$$\begin{aligned}\hat{T}_{el,n} &= \hat{S}_n + \hat{D}_n + \dots \\ &= \sum_{ai} s_{ai} E_{ai} + \sum_{aibj} d_{aibj} E_{ai} E_{bj} + \dots ,\end{aligned} \tag{4.35}$$

where the coupled double amplitudes d_{aibj} should not be confused with the dipole elements d_{pq}.

There are also a few alternative photon excitation operators which may yield interesting results. First of them is the canonical position operator $\hat{q} = \frac{1}{\sqrt{2\omega}}(\hat{b}^\dagger + \hat{b})$, which commutes with the dipole term, but not the photon number term. A disadvantage with this operator is that $\langle 0|\hat{q}^{2n}|0\rangle$ is generally not 0. With this, there are many more terms which must be calculated which, in principle, is more computationally expensive. A similar approach would be to use the "real" canonical momentum operator $i\hat{p} = \sqrt{\frac{\omega}{2}}(\hat{b}^\dagger - \hat{b})$, which would have the same disadvantage as $\hat{q}$. One interesting thing about $i\hat{p}$ is that the pure photon transformation $e^{-i\hat{p}}\hat{H}e^{i\hat{p}}$ is a coherent state transformation. The excited state terms would essentially be coherently transformed in a similar way to how the ground state is coherently transformed now, $e^{-i\hat{T}_{el}\hat{p}}He^{i\hat{T}_{el}\hat{p}}$.

4.3 Reference Wavefunction

For the reference wavefunction we will develop a QED formulation of Hartree-Fock, referred to as QED-HF. The QED-HF state is determined from the Fock matrix, which is found from the Hamiltonian averaged over the photon ground state. This is simply the photon vacuum $|0\rangle$,

$$\langle 0|\hat{H}|0\rangle = \hat{H}_e^{(0)} + c^{(0)} . \tag{4.36}$$

The Fock matrix is found in the same as way as in standard HF Eq. [3.29], but now it contains modified integrals,

$$F_{pq} = h_{pq}^{(0)} + \sum_i (2g_{pqii}^{(0)} - g_{piiq}^{(0)}) = F_{pq}^e + \beta\left(\sum_a d_{pa}d_{aq} - \sum_i d_{pi}d_{iq}\right). \tag{4.37}$$

Here F_{pq}^e is the HF electronic Fock matrix. The electronic state changes depending on the coupling strength and the dipole matrix elements. The QED-HF energy is

$$E_{\text{QED-HF}} = E_e + \beta \langle HF|\hat{d} - \langle d\rangle_{HF}|HF\rangle^2 . \tag{4.38}$$

The fluctuation of the dipole will interact with the field and increase the energy, even for molecules with a non-permanent dipole such as H_2 and CO_2. Since the Fock matrix is not the same as in standard HF, the electronic density will be modified and cause changes in E_e as well.

4.4 Ground State

In this section we will derive the QED-CC ground state equations. The QED extension to the projection equations are introduced before we do a perturbation analysis of QED-CC. Finally we will delve into the ground state equations of QED-CCS and QEC-CCSD. Many of the equations of QED-CCS are reused in QED-CCSD to simplify derivation as much as possible. The perturbation analysis is the foundation for approximating that the QED-CCSD coupled double amplitudes are small, $t_{\mu_2,n} \approx 0$, which will reduce the equation complexity significantly.

The projection equation of standard CC is

$$\Omega_\mu = \langle \overline{\mu} | \hat{H}^T | HF \rangle \, , \tag{4.39}$$

where $|\mu\rangle$ are the excited states created by the excitation operator $\hat{\tau}_\mu$. The excitation operators of QED-CC are of the form $\hat{\tau}_\mu$, $\hat{b}^{\dagger\, n}\hat{\tau}_\mu$ and $\hat{b}^{\dagger\, n}$. The extension of the projection equation in QED formalism is simple,

$$\Omega_\mu = \langle \overline{\mu}, 0 | \hat{H}^T | HF, 0 \rangle \, , \tag{4.40}$$

$$\Omega_{\mu,n} = \langle \overline{\mu, n} | \hat{H}^T | HF, 0 \rangle \, , \tag{4.41}$$

$$\Omega_n = \langle HF, \overline{n} | \hat{H}^T | HF, 0 \rangle \, . \tag{4.42}$$

The overline for photon states means normalized with respect to $\langle \overline{n} | \hat{b}^{\dagger\, n} | 0 \rangle = 1$. Here $\hat{T}$ is the QED excitation operator from the QED-CC ansatz, Eq. [4.33]. By expanding H^T using the BCH expansion, the explicit expression for the projection equations are obtained. The amplitudes are found by iteratively minimizing $\left\| \vec{\boldsymbol{\Omega}} \right\|$. The QED-CC ground state energy is obtained when projecting onto the $\langle HF, 0|$ state,

$$E_{\text{QED-CC}} = E_{\text{QED-HF}} + \sum_{aibj} \left(t_{ij}^{ab} + t_i^a t_j^b \right) (2g_{iajb} - g_{ibja}) + 2\alpha \sum_{ai} d_{ia} (s_{ai} + \gamma_1 t_{ai}) \, , \tag{4.43}$$

where s_{ai} are the coupled singles amplitudes and γ_1 is the one-photon amplitude. The energy only depends on the electronic single and double amplitudes, the coupled single amplitudes and the one-photon amplitudes. The main difference between the QED-CCSD is that the coupled singles amplitudes contribute to first order.

4.4.1 Perturbation Analysis

The Hamiltonian can be defined in terms of a Hamiltonian $\hat{H}_0$ with a known solution, and a perturbation $\hat{\Phi}$,

$$\hat{H} = \hat{H}_0 + \hat{\Phi} \, , \tag{4.44}$$

$$\hat{H}_0 = \hat{f} + \omega \hat{b}^\dagger \hat{b} + h_{\text{nuc}} \, , \tag{4.45}$$

$$\hat{\Phi} = \hat{H} - \hat{H}_0 = \hat{\Phi}_0 + \alpha (\hat{d} - \langle d \rangle)(\hat{b}^\dagger + \hat{b}) \, . \tag{4.46}$$

Here $\hat{f}$ is the Fock operator, which includes the dipole self-energy, and $\hat{\Phi}_0$ is the two-electron perturbation potential. Let $\hat{T}$ be the general excitation operator

$$\hat{T} = \hat{T}_0 + \sum_{n=1} \hat{T}_n \hat{b}^{\dagger n} + \sum_{n=1} \gamma_n \hat{b}^{\dagger n}, \tag{4.47}$$

we get the amplitude relations

$$t_{\mu,n}(\epsilon_\mu + n\omega) = -\langle \overline{\mu, n} | e^{-\hat{T}} \hat{\Phi} e^{\hat{T}} | HF, 0 \rangle \tag{4.48}$$

$$\gamma_n \omega = -\langle HF, \overline{n} | e^{-\hat{T}} \hat{\Phi} e^{\hat{T}} | HF, 0 \rangle . \tag{4.49}$$

Then in orders of perturbation,

$$t^{(0)}_{\mu,n}(\epsilon_\mu + n\omega) = 0 \tag{4.50}$$

$$t^{(1)}_{\mu,n}(\epsilon_\mu + n\omega) = -\langle \overline{\mu} | \hat{\Phi}_0 | HF \rangle \langle n|0\rangle - \langle \overline{\mu} | \alpha \hat{d} | HF \rangle \langle n|1\rangle \tag{4.51}$$

$$\begin{aligned} t^{(2)}_{\mu,n}(\epsilon_\mu + n\omega) = &-\langle \overline{\mu} | [\hat{\Phi}_0, \hat{T}_n] | HF \rangle - \langle \overline{\mu} | \left[\alpha \hat{d}, \hat{T}_{n-1} + n\hat{T}_n \right] | HF \rangle \\ &+ \langle \overline{\mu} | \alpha (n+1) (\hat{T}_{n+1} + \gamma_{n+1}) (\hat{d} - \langle d \rangle) | HF \rangle \end{aligned} \tag{4.52}$$

Single excitation do not contribute to $t^{(1)}_{\mu,0}$ because of the Brillouin theorem Eq. [3.26]. Therefore, similarly to standard CC, only double excitations contribute to the first order non-coupled amplitudes. The first order coupled amplitudes $t^{(1)}_{\mu,1}$ have only single excitation contributions. The photon amplitudes in orders of perturbations are

$$\gamma^{(0)}_n(n\omega) = 0 \tag{4.53}$$

$$\gamma^{(1)}_n(n\omega) = 0 \tag{4.54}$$

$$\gamma^{(2)}_n(n\omega) = -\langle HF | [\hat{\Phi}_0, \hat{T}_n] | HF \rangle - \langle HF | [\alpha \hat{d}, \hat{T}_{n-1} + n\hat{T}_n] | HF \rangle \tag{4.55}$$

The photon amplitudes only has contributions from orders 2 and up. Without the coherent state transformation, there would also be a first order contribution.

4.4.2 QED-CCS

In this section the ground state equations for QED-CCS are derived before they are used in QED-CCSD in the next section. In QED-CCS the excitation operator is

$$\exp(\hat{T}_S) = \exp(\hat{T}_1) \exp\left(\sum_{n=1} \hat{S}_n \hat{b}^{\dagger n} \right) \exp\left(\sum_{m=1} \gamma_m \hat{b}^{\dagger m} \right). \tag{4.56}$$

The $\hat{T}_1$ transformation is known to only change the integrals[23], but we will reproduce the result together with the $\hat{S}_n \hat{b}^{\dagger n}$ and $\hat{b}^{\dagger n}$ transformation here.

$\hat{\mathbf{T}}_1$ Transformation

First consider the one-electron operator $\hat{h}$ commutator for $\hat{T}_1$,

$$\left[\sum_{pq} h_{pq}E_{pq}, \sum_{ai} t_{ai}E_{ai}\right] = \sum_{pqai} h_{pq}t_{ai}[E_{pq}, E_{ai}] \quad [4.57]$$

$$= \sum_{pai} h_{pa}t_{ai}E_{pi} - \sum_{qai} t_{ai}h_{iq}E_{aq} \quad [4.58]$$

$$= \sum_{pq} [\mathbf{h}, \mathbf{t}]_{pq}E_{pq} \quad [4.59]$$

where we have set t_{pq} to be a matrix of t_{ai} which is non-zero only for the virtual-occupied elements,

$$t_{pq} = t_{pq} \quad \text{if} \quad p \text{ virtual, } q \text{ occupied} \quad [4.60]$$

$$t_{pq} = 0 \quad \text{else} \quad [4.61]$$

We may now show that a $\hat{T}_1$ transformation only shifts the integrals,

$$e^{-\hat{T}_1}\left(\sum_{pq} h_{pq}E_{pq}\right)e^{\hat{T}_1} = \sum_{pq}(h_{pq} + [\mathbf{h}, \mathbf{t}]_{pq} + \frac{1}{2}[[\mathbf{h}, \mathbf{t}], \mathbf{t}]_{pq})E_{pq} \quad [4.62]$$

$$= \sum_{pq} h^{t1}_{pq}E_{pq} \quad [4.63]$$

Similarly we may calculate the commutator for the two-electron integrals,

$$\left[\sum_{pqrs} g_{pqrs}e_{pqrs}, \sum_{ai} t_{ai}E_{ai}\right] = \sum_{pqrsai} g_{pqrs}t_{ai}[e_{pqrs}, E_{ai}] \quad [4.64]$$

$$= \sum_{pqrs} [\mathbf{g}, \mathbf{t}]_{pqrs}e_{pqrs} \quad [4.65]$$

Here we have defined the commutator between a 4-index matrix g_{pqrs} and 2-index matrix t_{pq} as

$$[\mathbf{g}, \mathbf{t}]_{pqrs} = \sum_{u} \left(g_{purs}t_{uq} - t_{pu}g_{uqrs} + g_{pqru}t_{us} - t_{ru}g_{pqus}\right). \quad [4.66]$$

This is the same as commuting the two leftmost indices of g with t plus the commutator with the two rightmost indices. Now we may show that a $\hat{T}_1$ transformation only shifts the two electron integrals as well,

$$e^{-T_1}\left(\sum_{pqrs} g_{pqrs}e_{pqrs}\right)e^{T_1} = \sum_{pqrs}\left(g_{pqrs} + [\mathbf{g}, \mathbf{t}]_{pqrs} + \frac{1}{2!}[[\mathbf{g}, \mathbf{t}], \mathbf{t}]_{pqrs}\right.$$
$$\left. + \frac{1}{3!}[[[\mathbf{g}, \mathbf{t}], \mathbf{t}], \mathbf{t}]_{pqrs} + \frac{1}{4!}[[[[\mathbf{g}, \mathbf{t}], \mathbf{t}], \mathbf{t}], \mathbf{t}]_{pqrs}\right)e_{pqrs}, \quad [4.67]$$

$$= \sum_{pqrs} g^{t1}_{pqrs} e_{pqrs} \,. \qquad [4.68]$$

In summary, the $\hat{T}_1$ transformation only shifts the one-and two-electron integrals,

$$e^{-\hat{T}_1} H e^{\hat{T}_1} = \sum_{n=0}^{1} \hat{b}^{\dagger n} \left(H_e^{t1,(n)} + c^{(n)} \right) + \alpha \left(\sum_{n}^{0} \hat{b}^{\dagger n} \hat{d}^{t1,(n)} - \langle d \rangle \right) \hat{b} + \omega \hat{b}^\dagger \hat{b} \qquad [4.69]$$

$\hat{S}_n \hat{b}^{\dagger n}$ Transformation

The argument for the $\hat{S}_n \hat{b}^{\dagger n}$ transformation is similar to $\hat{T}_1$, except now each commutator also has a photon excitation $\hat{b}^\dagger$. We only show the shift in integral for the one-electron operator because the shift for the two-electron integral are trivially similar.

$$\begin{aligned} \exp\left(- \sum_n \hat{S}_n \hat{b}^{\dagger n} \right) \left(\sum_{pq} h_{pq} E_{pq} \right) \exp\left(\sum_n \hat{S}_n \hat{b}^{\dagger n} \right) = \\ \sum_{pq} \left(h_{pq} + \sum_n \hat{b}^{\dagger n} [h, s_n]_{pq} + \frac{1}{2} \sum_{nm} \hat{b}^{\dagger n+m} [[h, s_n], s_m]_{pq} \right) E_{pq} \end{aligned} \qquad [4.70]$$

This makes contributions up to twice the number of photons included in the sum, N_p. N_p should be infinite in an exact calculation, but will be restricted when doing computations. The one-electron integrals make contributions up to $\hat{b}^{\dagger 2N_p}$. The two-electron integrals make contributions up to $\hat{b}^{\dagger 4N_p}$ due to there being up to 4 commutators as seen in Eq. [4.67]. The transformation also transforms two $\hat{b}$ terms,

$$\exp\left(- \sum_n \hat{S}_n \hat{b}^{\dagger n} \right) \hat{b} \exp\left(\sum_n \hat{S}_n \hat{b}^{\dagger n} \right) = \hat{b} + \sum_{n=1} \hat{S}_n \hat{b}^{\dagger n-1} n \qquad [4.71]$$

The $\hat{S}_n \hat{b}^{\dagger n}$ transformed Hamiltonian may be written as

$$\begin{aligned} \exp\left(- \sum_n \hat{S}_n \hat{b}^{\dagger n} \right) \hat{H} \exp\left(\sum_n \hat{S}_n \hat{b}^{\dagger n} \right) = \sum_{n=0}^{4N_p} \hat{b}^{\dagger n} \left(\hat{H}_e^{(n)} + c^{(n)} \right) \\ + \alpha \left(\sum_{n=0}^{2N_p} \hat{b}^{\dagger n} \hat{d}^{(n)} - \langle d \rangle \right) \hat{b} + \omega \hat{b}^\dagger \hat{b} \,, \end{aligned} \qquad [4.72]$$

where $h^{(n)}$, $g^{(n)}$, $d^{(n)}$, have been redefined using the BCH expansion.

$\hat{\mathbf{b}}^{\dagger\,\mathbf{n}}$ Transformation

Finally, the $\gamma_n \hat{b}^{\dagger\, n}$ transformation only transforms terms with $\hat{b}$,

$$\exp\Big(-\sum_n \gamma_n \hat{b}^{\dagger\, n}\Big)\hat{b}\exp\Big(\sum_n \gamma_n \hat{b}^{\dagger\, n}\Big) = \hat{b} + \sum_{n=1} \gamma_n \hat{b}^{\dagger\, n-1} n. \tag{4.73}$$

The transformed Hamiltonian may then be written

$$\begin{aligned}\exp\Big(-\sum_n \gamma_n \hat{b}^{\dagger\, n}\Big)\hat{H}\exp\Big(\sum_n \gamma_n \hat{b}^{\dagger\, n}\Big) = \sum_{n=0}^{N_p} \hat{b}^{\dagger\, n}\Big(\hat{H}_e^{(n)} + c^{(n)}\Big) \\ + \alpha\Big(\sum_{n=0}^{0} \hat{b}^{\dagger\, n}\hat{d}^{(n)} - \langle d\rangle\Big)\hat{b} + \omega\hat{b}^\dagger\hat{b}\,,\end{aligned} \tag{4.74}$$

where $h^{(n)}$ and $c^{(n)}$ have been redefined.

One-Photon Transformation

In summary, the QED-CCS transformation with and without photons only transform the integrals of the Hamiltonian in Eq. [4.30]. Therefore, any expression derived with this Hamiltonian, where we do not restrict the sum, will also be true for the QED-CCS transformed Hamiltonian.

We will here show the Hamiltonian for one photon in QED-CCS, which can be reused in QED-CCSD. We transform the Hamiltonian using

$$\hat{T} = \hat{T}_1 + \hat{S}_1\hat{b}^\dagger + \gamma\hat{b}^\dagger\,. \tag{4.75}$$

Using the BCH expansion the transformed Hamiltonian may be written as

$$e^{-\hat{T}}\hat{H}e^{\hat{T}} = \sum_{n=0}^{4} \hat{b}^{\dagger\, n}\Big(\hat{H}_e^{(n)} + c^{(n)}\Big) + \alpha\Big(\sum_{n=0}^{2} \hat{b}^{\dagger\, n}\hat{d}^{(n)} - \langle d\rangle\Big)\hat{b} + \omega\hat{b}^\dagger\hat{b}\,, \tag{4.76}$$

where electron integrals are $\hat{T}_1$ transformed. We have redefined the one- and two-electron integrals, and the constant terms c,

$$h_{pq}^{(0)} = h_{pq}^{t1} + \beta(d^2)_{pq}^{t1} - 2\beta\langle d\rangle d_{pq}^{t1} - \alpha\langle d\rangle s_{pq} + \alpha(ds)_{pq}^{t1} + \gamma\alpha d_{pq}^{t1} \tag{4.77}$$

$$h_{pq}^{'(1)} = \alpha d_{pq}^{t1} + \omega s_{pq} \tag{4.78}$$

$$g_{pqrs}^{(0)} = g_{pqrs}^{t1} + 2\beta(d_{pq}d_{rs})^{t1} + \alpha(d_{pq}s_{rs} + s_{pq}d_{rs})^{t1} \tag{4.79}$$

$$c^{(0)} = h_{nuc} + \beta\langle d\rangle^2 \tag{4.80}$$

$$c^{(1)} = \omega\gamma - \alpha\langle d\rangle \tag{4.81}$$

Here both h and $h^{'}$ contribute to the one-electron integrals in $\hat{H}_e$. Higher order one-

electron terms are calculated from

$$h_{pq}^{(n)} = \frac{1}{n!}[\mathbf{h}^{(n-1)}, \mathbf{s}]_{pq}, \tag{4.82}$$

$$h_{pq}^{'(n)} = \frac{1}{(n-1)!}[\mathbf{h}'^{(n-1)}, \mathbf{s}]_{pq}, \tag{4.83}$$

where h terminates for $n > 2$ and $h^{'}$ for $n > 3$ because $\mathbf{s}^2 = 0$. Higher order two-electron terms are calculated from

$$g_{pqrs}^{(n)} = \frac{1}{n!}[\mathbf{g}, \mathbf{s}]_{pqrs} \tag{4.84}$$

which terminates for $n > 4$.

4.4.3 QED-CCSD

In QED-CCSD we include the double excitations into the excitation operator,

$$\hat{T} = \hat{T}_1 + \hat{S}_1\hat{b}^\dagger + \gamma\hat{b}^\dagger + \hat{T}_2 + \hat{D}_1\hat{b}^\dagger \tag{4.85}$$

where $\hat{D}_1$ is a doubles excitation. To reduce the complexity of the QED-CCSD equations, we will assume that d_{aibj} amplitudes are approximately zero. This is because the coupled double amplitudes are zero to first order in the perturbation, as seen in Eq. [4.51]. From this approximation, we may reduce the number of excitations to only $\hat{T}_2$ by using the QED-CCS transformed Hamiltonian in Eq. [4.76], referred to as $\hat{H}_S$. To get an expression to determine all the amplitudes, we need to project onto all the excited states produces by the excitation operators,

$$\{\langle\overline{\mu}, 0|, \langle\overline{\mu_1, n}|, \langle HF, \overline{n}|\} \tag{4.86}$$

where μ is an electronic excited state, μ_1 is a singly electronically excited state, and $n > 0$. The purely electronic projection equation is simple,

$$\Omega_{\mu,0} = \left\langle\overline{\mu, 0}\middle|e^{-\hat{T}_2}\hat{H}_S e^{\hat{T}_2}\middle|HF, 0\right\rangle = \langle\overline{\mu}|e^{-\hat{T}_2}\hat{H}_e^{(0)}e^{\hat{T}_2}|HF\rangle\ , \tag{4.87}$$

$$\Omega_{\mu_1,n} = \langle\overline{\mu_1, n}|e^{-\hat{T}_2}\hat{H}_S e^{\hat{T}_2}|HF, 0\rangle = \langle\overline{\mu_1}|e^{-\hat{T}_2}\hat{H}_e^{(n)}e^{\hat{T}_2}|HF\rangle\ . \tag{4.88}$$

These are the same projection equation as for standard CC theory with redefined integrals. The photon projections are similar to the CCSD energy,

$$\Omega_{HF,n} = \langle HF, \overline{n}|e^{-\hat{T}_2}\hat{H}_S e^{\hat{T}_2}|HF, 0\rangle = \langle HF|e^{-\hat{T}_2}\hat{H}_e^{(n)}e^{\hat{T}_2}|HF\rangle + c^{(n)}. \tag{4.89}$$

Minimizing the projection equations Eq. (4.87, 4.88, 4.89) will determine the ground state. The energy can be calculated from Eq. [4.43].

4.5 Excited States

To find the excited states for QED-CCSD, we will use the CC Equation of Motion approach (EOM). The excitation energies from the ground state are found from diagonalizing the Jacobian matrix, A. We will choose a projection basis,

$$\{\langle\overline{\mu}, 0|\,, \langle\overline{\mu, n}|\,, \langle HF, \overline{n}|\}. \tag{4.90}$$

This basis includes $\langle\overline{\mu_2, n}|$, and is bigger than the projection basis we used to solve the ground state equations, Eq. [4.86]. Looking at the full QED-CCSD Hamiltonian matrix, including the ground state in the projection basis,

$$\mathbf{H} = \begin{bmatrix} E_0 & \vec{\boldsymbol{\eta}} \\ \vec{\boldsymbol{\Omega}} & \mathbf{A} + E_0\mathbf{I} \end{bmatrix} \tag{4.91}$$

Generally in CC, all the projection equations are fulfilled, thus $\vec{\boldsymbol{\Omega}}$ is zero. Then the eigenvalues of $\mathbf{A}$ may be interpreted as excitation energies. We assume that the amplitudes from the double excitations are small, as they only have second order contributions in the perturbation as seen in Eq. [4.51]. Therefore, $\vec{\boldsymbol{\Omega}}$ should be small even if the coupled-double amplitudes effectively are zero. This is an important assumption to make in order to reduce the complexity of the equations and it ensures that the eigenvalues of the Jacobian is equivalent to the excitation energies.

The equations for the CCSD Jacobian are long and many. We will try to derive the Jacobian equation for QED-CCSD in such a way that we can reuse many of the expression already present and verified in many CCSD implementations. We start out with writing the Jacobian in the EOM,

$$A_{\mu n,\nu m} = \langle \mu, n|e^{-\hat{T}_2}[\hat{H}_S, \tau_\nu \hat{b}^{\dagger\, m}]e^{\hat{T}_2}|HF, 0\rangle\ , \tag{4.92}$$

where $\hat{\tau}$ is an excitation operator, $\hat{\tau}_\nu\,|HF\rangle = |\nu\rangle$, and $n, m \geq 0$. We will first consider $\langle\overline{n}|\,[\hat{H}_S,\ \hat{\tau}]\,|0\rangle$,

$$\langle\overline{n}|\,[\hat{H}_S, \hat{\tau}_\nu]\,|0\rangle = [\hat{H}_e^{(n)}, \hat{\tau}_\nu] \tag{4.93}$$

$$\langle\overline{n}|\,[\hat{H}_S, \hat{b}^\dagger]\,|0\rangle = \alpha\Big(\hat{d}^{(n)} - \langle d\rangle\,\delta_{n0}\Big) + \omega\delta_{n1} \tag{4.94}$$

$$\langle\overline{n}|\,[\hat{H}_S, \hat{\tau}_\nu\hat{b}^\dagger]\,|0\rangle = \langle\overline{n}|\,\hat{b}^\dagger[\hat{H}_S, \hat{\tau}_\nu]\,|0\rangle + \langle\overline{n}|\,\hat{\tau}_\nu[\hat{H}_S, \hat{b}^\dagger]\,|0\rangle + \langle\overline{n}|\,[[\hat{H}_S, \hat{b}^\dagger], \hat{\tau}_\nu]\,|0\rangle \tag{4.95}$$

$$= [\hat{H}_e^{(n-1)} + \alpha\hat{d}^{(n)}, \hat{\tau}_\nu] + \hat{\tau}_\nu\alpha\Big(\hat{d}^{(n)} - \langle d\rangle\,\delta_{n0}\Big) + \hat{\tau}_\nu\omega\delta_{n1} \tag{4.96}$$

where $\hat{H}_e^{(-1)} = 0$. We split the Jacobian into two parts,

$$\mathbf{A} = \mathbf{A}^{\mathrm{el}} + \mathbf{A}^{\mathrm{ph}} \tag{4.97}$$

where $\mathbf{A}^{\mathrm{el}}$ contains terms that will be simplified due to their similarity to standard CC,

and $\mathbf{A}^{\text{ph}}$ containing the rest of the terms,

$$\mathbf{A}^{\text{el}} = \begin{bmatrix} [\hat{H}_e^{(0)}, \hat{\tau}_\nu] & [\alpha\hat{d}^{(0)}, \tau_\nu] & \alpha d^{(0)} \\ [\hat{H}_e^{(1)}, \hat{\tau}_\nu] & [\hat{H}_e^{(0)} + \alpha\hat{d}^{(1)}, \tau_\nu] & \alpha d^{(1)} \\ [\hat{H}_e^{(1)}, \hat{\tau}_\nu] & [\hat{H}_e^{(0)} + \alpha\hat{d}^{(1)}, \tau_\nu] & 0 \end{bmatrix} \tag{4.98}$$

Here the projection is implicit. The left projection for each row is a different basis of [4.90] with $e^{-\hat{T}_2}$, for instance $\langle\overline{\mu}, 0| e^{-\hat{T}_2}$. The right side projection is the same for all rows and columns, $e^{\hat{T}_2}|HF, 0\rangle$.

We will try to simplify $\mathbf{A}^{\text{el}}$ as much as possible. By defining $\mathbf{A}_{00}^{\text{SD}}$, $\mathbf{A}_{10}^{\text{SD}}$, $\mathbf{A}_{01}^{\text{SD}}$ and $\mathbf{A}_{11}^{\text{SD}}$ as the standard CCSD expressions with different two-electron integrals g and Fock matrices F, all commutators with $\hat{\tau}_\nu$ may be simplified to $\mathbf{A}^{\text{SD}}$. The bottom row may also be simplified by relating it to the CCSD $\vec{\boldsymbol{\eta}}$, using $|HF\rangle\,\hat{\tau}_\nu = 0$,

$$\langle HF|[\hat{H}_e, \hat{\tau}_\nu]|HF\rangle = \langle HF|\hat{H}_e|\nu\rangle = \eta_\nu^{SD}. \tag{4.99}$$

The right column may be simplified by relating them to the CCSD projection equations $\vec{\boldsymbol{\Omega}}$. This gives a much simplified Jacobian,

$$\mathbf{A}^{\text{el}} = \begin{bmatrix} \mathbf{A}_{00}^{\text{SD}} & \mathbf{A}_{01}^{\text{SD}} & \vec{\boldsymbol{\Omega}}_0^{\text{SD}} \\ \mathbf{A}_{10}^{\text{SD}} & \mathbf{A}_{11}^{\text{SD}} & \vec{\boldsymbol{\Omega}}_1^{\text{SD}} \\ \vec{\boldsymbol{\eta}}_0^{\text{SD}} & \vec{\boldsymbol{\eta}}_1^{\text{SD}} & 0 \end{bmatrix} \tag{4.100}$$

where the implicit projection has been removed. The Fock matrices and two-electron integrals used to calculate the different CCSD expressions are given in Table 4.1. Now we want to simplify $\mathbf{A}^{\text{ph}}$ as much as possible,

$$\mathbf{A}^{\text{ph}} = \begin{bmatrix} 0 & \hat{\tau}_\nu(\alpha\hat{d}^{(0)} - \alpha\langle d\rangle) & 0 \\ 0 & \hat{\tau}_\nu(\alpha\hat{d}^{(1)} + \omega) & 0 \\ 0 & 0 & \alpha d^{(1)} + \omega \end{bmatrix} \tag{4.101}$$

First we consider the terms containing only $\hat{\tau}_\nu$,

$$\langle\overline{\mu}|e^{-\hat{T}_2}\tau_\nu e^{\hat{T}_2}|HF\rangle = \delta_{\mu\nu}. \tag{4.102}$$

The bottom-right photon-photon term,

$$\langle HF|e^{-\hat{T}_2}\alpha\hat{d}^{(1)} + \omega e^{\hat{T}_2}|HF\rangle = 2\alpha\sum_i d_{ii}^{(1)} + \omega. \tag{4.103}$$

The two final terms in the middle column are both of the form

$$\alpha\langle\overline{\mu}|\hat{\tau}_\nu e^{-\hat{T}_2}\hat{d}^{(n)}e^{\hat{T}_2}|HF\rangle. \tag{4.104}$$

First we note that a single excitation on the double excited projected state produces a single excitation,

$$\left\langle \overline{\substack{ab \\ ij}} \right| \hat{\tau}_{ck} = \delta_{ai,ck} \left\langle \overline{\substack{b \\ j}} \right| + \delta_{bj,ck} \left\langle \overline{\substack{a \\ i}} \right| \quad [4.105]$$

We will expand Eq. [4.104] in the basis $\{|\mu_1\rangle, |\mu_2\rangle\}$,

$$\begin{bmatrix} \delta_{\mu_1\nu_1} 2\alpha \sum_i d_{ii}^{(n)} & 0 \\ \Omega_{bj,n}^{\mathrm{SD,ss}} \delta_{ai,\nu_1} + \Omega_{ai,n}^{\mathrm{SD,ss}} \delta_{bj,\nu_1} & \delta_{\mu_2\nu_2} 2\alpha \sum_i d_{ii}^{(n)} \end{bmatrix} \quad [4.106]$$

where $\mu_2 = aibj$, and $\Omega^{\mathrm{SD,ss}}$ is the CCSD Ω contribution from single excitations to the singly excited state calculated using $F_{pq} = \alpha d_{pq}$ and $g = 0$ (Table 4.1). With this we have all of the elements in the Jacobian, and may start calculating the excitation energies.

To sum up, we assume that the coupled doubles amplitudes are zero. In this way we can calculate most of the terms in QED-CCSD using CCSD methods. The Jacobian matrix is given by

$$\mathbf{A} = \begin{bmatrix} \mathbf{A}_{00}^{\mathrm{SD}} & \mathbf{A}_{01}^{SD} & \vec{\mathbf{\Omega}}_0^{\mathrm{SD}} \\ \mathbf{A}_{10}^{\mathrm{SD}} & \mathbf{A}_{11}^{SD} & \vec{\mathbf{\Omega}}_1^{\mathrm{SD}} \\ \vec{\boldsymbol{\eta}}_0^{\mathrm{SD}} & \vec{\boldsymbol{\eta}}_1^{\mathrm{SD}} & 0 \end{bmatrix} + \begin{bmatrix} 0 & \hat{\tau}_\nu \alpha \hat{d}^{(0)} - \hat{\tau}_\nu \alpha \langle d \rangle & 0 \\ 0 & \hat{\tau}_\nu \alpha \hat{d}^{(1)} + \hat{\tau}_\nu \omega & 0 \\ 0 & 0 & \alpha d^{(1)} + \omega \end{bmatrix} \quad [4.107]$$

and its eigenvalues are the excitation energies. The methods to calculate the different elements in this Jacobi matrix are given in Table 4.1 and Eqs. (4.102, 4.103, 4.106).

Table 4.1 / Fock matrices F_{pq} and two-electron integrals g_{pqrs} used to calculate different CCSD expressions in QED-CCSD.

	F_{pq}	g_{pqrs}
$\mathbf{A}_{00}^{\mathrm{SD}}$	$F_{pq}^{(0)}$	$g_{pqrs}^{(0)}$
$\mathbf{A}_{01}^{\mathrm{SD}}$	$\alpha d_{pq}^{(0)}$	0
$\mathbf{A}_{10}^{\mathrm{SD}}$	$F_{pq}^{(1)}$	$g_{pqrs}^{(1)}$
$\mathbf{A}_{11}^{\mathrm{SD}}$	$F_{pq}^{(0)} + \alpha d_{pq}^{(1)}$	$g_{pqrs}^{(0)}$
$\vec{\boldsymbol{\eta}}_0^{\mathrm{SD}}$	$F_{pq}^{(1)}$	$g_{pqrs}^{(1)}$
$\vec{\boldsymbol{\eta}}_1^{\mathrm{SD}}$	$F_{pq}^{(0)} + \alpha d_{pq}^{(1)}$	$g_{pqrs}^{(0)}$
$\vec{\mathbf{\Omega}}_0^{\mathrm{SD}}$	$\alpha d_{pq}^{(0)}$	0
$\vec{\mathbf{\Omega}}_1^{\mathrm{SD}}$	$\alpha d_{pq}^{(1)}$	0
$\vec{\mathbf{\Omega}}_n^{\mathrm{SD},ss}$	$\alpha d_{pq}^{(n)}$	0

Rest of this page intentionally left blank.

Chapter 5

Results and Discussion

QED-CC allows for the calculation of coupled light-matter systems. We have implemented QED-CC in a development version of the eT software package[49]. First, we will look at the results for diatomic molecules to test the program and better understand the effects introduced by strong light-matter interaction. To showcase some of the effects that strong light-matter coupling may induce, we have calculated optical spectra varying the bond-length, cavity frequency, and coupling. In addition to this, we show that the equilibrium geometry is dependent on the coupling strength, and that the translation invariance is fulfilled. Then, we will apply the code to a realistic scenario, which in our case is the charge transfer state in p-nitroaniline (PNA), which serves as a precursor for dyes in photovoltaic applications. The charge transfer state in PNA has been studied extensively in solution[50, 51], but this is the first, although simple, study of PNA inside a cavity in a vacuum.

5.1 Tests on Diatomic Molecules

In this section, we will compare QED-CCSD against an exact reference, QED-FCI. QED-FCI refers to diagonalizing the Hamiltonian in the space of all configurations, which is exact within the truncated basis. The dispersion of the QED-CCSD spectra with the cavity frequency and their dependence on the coupling strength and bond-length has been investigated here. This was done for the non-polar H_2 and the polar HF molecules. Finally, we will show numerically that our implementation respects the translational invariance of the Hamiltonian for a charged molecule.

A comparison between the ground state and excited state energies of H_2 for QED-CCSD against QED-FCI is shown in Table 5.1. From the table, we see that including photons at a mean-field level increases the energy. Because H_2 has no permanent dipole, this shift in energy is purely due to the dipole self-energy d^2 term, which for experimental coupling values is a quite small effect. QED-CCS has an energy which is similar to QED-HF, only slightly higher. This is unlike the non-QED scenario, where CCS has the same energy as HF. This is an effect of the coupled single excitations $\hat{S}_1\hat{b}^\dagger$ present

Table 5.1 / Ground state (GS) and excited state (ES) energies in atomic units for H_2 in 3-21G at $R = 1$ Å, $\lambda = 0.05$, $\omega_{cav} = 0.5$ with one photon. QED-FCI(3) is calculated with three photons. Δ is the difference in energy between QED-CCSD and QED-FCI(1).

Method	GS	ES1	ES2	ES3
HF	−1.091 386			
QED-HF	−1.089 578			
QED-CCS	−1.087 723	−0.637 960	−0.556 615	
QED-CCSD	−1.121 948	−0.656 237	−0.581 107	−0.298 597
QED-FCI(1)	−1.121 964	−0.653 460	−0.582 228	−0.298 462
QED-FCI(3)	−1.121 970	−0.655 012	−0.583 204	−0.299 850
Δ $[10^{-3}]$	0.016	2.8	−1.1	0.14

in QED-CCS. The accuracy is on the order 10^{-2} au, similar to the QED-HF ground state. Introducing QED-CCSD recovers most of the correlation energy. Due to the approximation on the coupled doubles of QED-CCSD, it cannot be exact for H_2. The accuracy of QED-CCSD on the ground and excited states are of the order 10^{-5} and 10^{-3} au respectively. We would expect the accuracy of the excited states to be similar to the ground state accuracy, indicating the possibility of a bug in the code. Due to time constraints, this could not be debugged properly. In order to recover all the correlation energy, we would need to properly include the coupled double excitation, $\hat{b}^\dagger \hat{T}_2$. This will ensure that the energies are exact within the truncated photon space for H_2.

In Figure 5.1 we show the energy spectrum as a function of ω_{cav} for QED-CCSD and QED-FCI. The contour in the background of the plots are the QED-FCI energies weighted by the intensity of the transition. The lines correspond to QED-CCSD excitation energies, where the color was determined by the norm of the electronic amplitudes $\|t_{el}\|$. The red diagonal lines represent photon lines coming from one of the blue electronic states. In this case, the calculations were run with only one photon, meaning that we see one photon line per electronic state. At the non-crossing intersections between the photon lines and electronic states, we have polaritons as indicated by the yellow color. At these points the states cannot be described purely by electronic and photon states separately, but rather as a combination. The width of the splitting corresponds to the Rabi splitting, Ω_R. We see that even though the numerical results for this version of QED-CCSD is not exact, we can reproduce the features of QED-FCI with great accuracy.

Figures 5.2 and 5.3 show a detailed analysis of the QED-CCSD potential energy surfaces and GS equilibrium bond distances as a function of the cavity frequency and coupling strength, performed for H_2 and HF respectively. For H_2 an aug-cc-pVDZ basis was used, while in this case the augmented functions have been neglected for HF (cc-pVDZ).

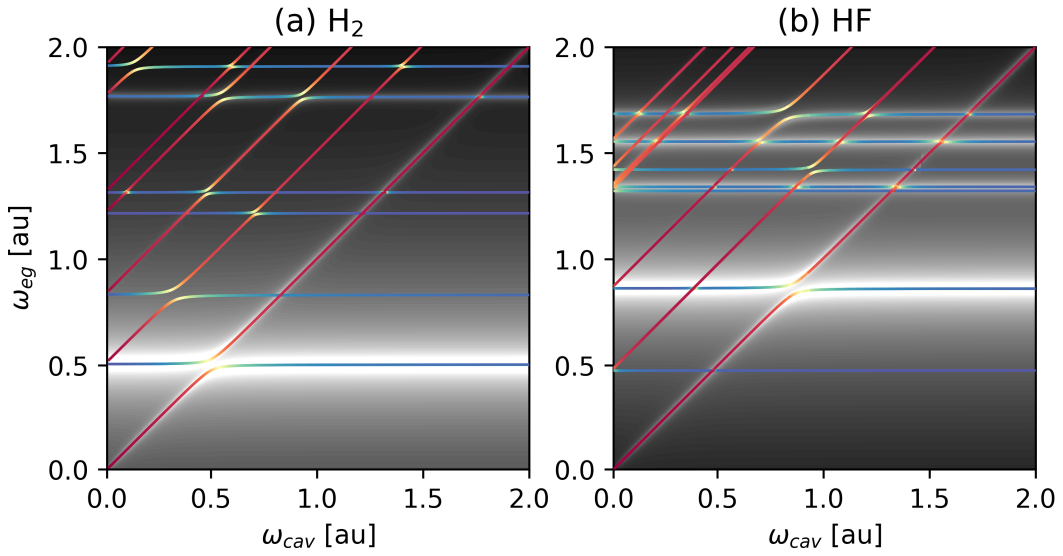

Figure 5.1 / Excitation energies ω_{eg} at different cavity frequencies ω_{cav} using coupling $\lambda = 0.05$. This was calculated using QED-CCSD (lines) and QED-FCI (background). For QED-CCSD, red indicate photon, yellow polariton and blue electronic states. The QED-FCI contours are scaled by the logarithm of the intensity, given in black and white. (a) H_2 with bond-radii $R = 1$ Å in 3-21G (b) HF with bond-radii $R = 0.917$ Å in STO-6G.

In all cases, only one photonic state was included in the calculation.

The energy spectrum with respect to cavity frequency, see Figures 5.2 (a) and 5.3 (a), show the strong interaction between the photon line from the ground state and the zero photon excited states. Here the yellow color indicate a interaction in the form of a polariton. The photon lines from the excited states also interact with the other zero photon excited states. Some excited states have also a small polaritonic character as $\omega_{cav} \to 0$, especially the states around -0.7 au for H_2. If the dipole of the excited state is not the same as the ground state, it will interact with the field in the cavity via the bi-linear coupling term $(\hat{d} - \langle d \rangle)(\hat{b}^\dagger + \hat{b})$ and get a polaritonic character. The spectrum with respect to the coupling strength is shown in Figures 5.2 (b) and 5.3 (b). Increasing the coupling strength also increases the Rabi splitting in the excited states. Due to the different transition dipole moments between the states, their order can be inverted. Increasing the coupling strength also increases the hybridization of the electronic and photonic states. This can be exploited to manipulate the properties of the states. It is interesting pointing out that at sufficiently high coupling, also the ground state of H_2 acquires a slight polaritonic character, clearly shown in Figure 5.2 (b) by the ground state line turning from blue to green. This hints at the prospect of changed ground state properties. For the couplings strengths studied here, the bilinear coupling is usually dominant. For larger coupling strengths, the dipole self-energy will dominate and produce a shift in energy of all the states.

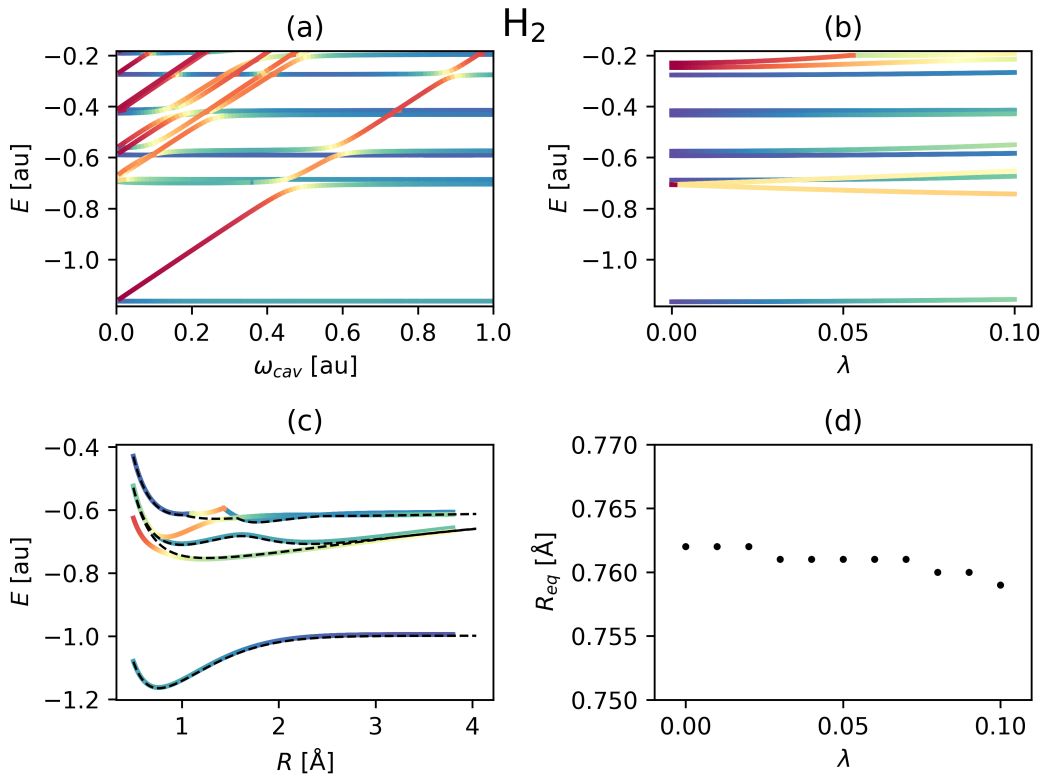

Figure 5.2 / QEC-CCSD calculations of H_2 in aug-cc-pVDZ basis with 1 photon. Blue indicates electronic state, red photon and yellow polariton. (a) The energy spectrum at different cavity frequencies at coupling $\lambda = 0.05$. (b) Energy spectrum for different couplings in a resonant cavity. (c) Potential energy surface in a resonant cavity at $\lambda = 0.05$ (d) Equilibrium bond-length R_{eq} at different couplings in a resonant cavity.

In Figures 5.2 (c) and 5.3 (c) we show a comparison of the potential energy surfaces with (colored solid line) and without (dashed black line) the coupling. The coupling to the cavity first of all generates new polaritonic energy surfaces in resonant condition. The polariton appears around the equilibrium bond-length with the first excited state. At increased bond-lengths, the photons also couple to the third electronic excited state, creating a pathway between the lower excited state and higher excited state. This clearly modifies the potential energy landscape, with possible significant implications on the photochemistry of the system.

Lastly, we show that also the ground state equilibrium geometry is dependent on the coupling strength (Figure 5.2, 5.3 (d)). With increased coupling values, the bond-length seems to decrease, opening possibilities to modifications of the system's chemical reactivity and electronic properties. This effect is also discussed by Hertzog *et al*[42]. However, the observed variations are quite small, even for relatively strong coupling values.

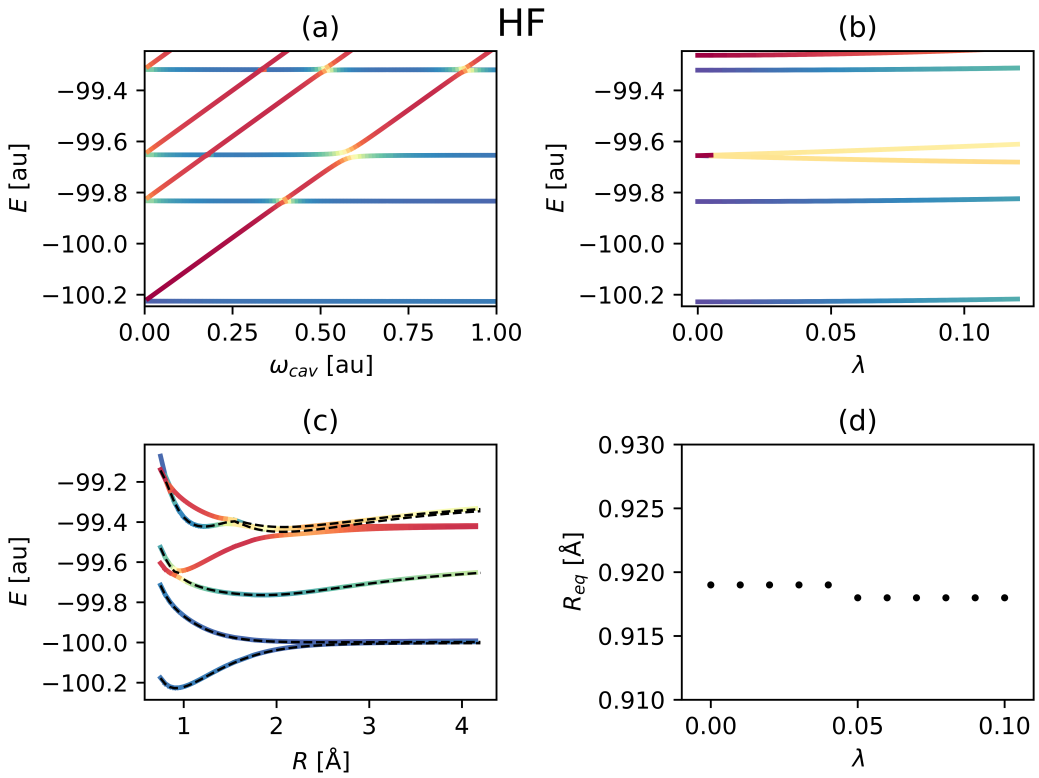

Figure 5.3 / QEC-CCSD calculations of HF in cc-pVDZ basis with 1 photon. Blue indicates electronic state, red photon and yellow polariton. (a) The energy spectrum at different cavity frequencies at coupling $\lambda = 0.05$. (b) Energy spectrum for different couplings in a resonant cavity. (c) Potential energy surface in a resonant cavity at $\lambda = 0.05$ (d) Equilibrium bond-length R_{eq} at different couplings in a resonant cavity.

Table 5.2 / Dipole, ground state energy (GS) and excitation energies (ES) of $NeLi^+$ centered at 0 Å and 10 Å. Calculated using one photon QED-CCSD with cavity frequency $\omega_{cav} = 1$, coupling $\lambda = 0.05$, bond length $R = 1$ Å in cc-pVDZ.

	0 Å	10 Å
Dipole [D]	2.273 742 020	50.305 778 332
GS	−135.505 216 535	−135.505 216 535
ES1	0.696 758 047	0.696 758 047
ES2	0.767 307 211	0.767 307 211
ES3	0.767 307 211	0.767 307 211
ES4	0.777 117 832	0.777 117 832

In Section 4.1.1, we proved analytically that our Hamiltonian is translation invariant. Here we want to prove it numerically for a test case. This effect is easily tested for charged molecules, where the dipole is not invariant to translation. For this reason we chose $NeLi^+$ as our test molecule. The energies for this system is shown in Table 5.2. These results clearly show that the electromagnetic field, through the use of coherent states, recover the translation invariance even for a large changes in the dipole moment. This is not a trivial feature to obtain in our implementation, because the modified one- and two-electron integrals are not independently translationally invariant. They only cancel each other when calculating the ground state energy and excitation energies.

5.2 Application on a Larger Molecule (PNA)

p-nitroaniline (PNA) is an aromatic molecule, see Figure 5.4a, that is used as a prototype for organic dyes commonly used in dye-sensitized solar cells for photovoltaic applications. Several groups have already studied PNA's charge transfer state in solution using time-dependent DFT[50, 51]. We will here study the coupling of a resonant cavity to the PNA charge transfer state. In this case QED-CCSD was used to calculate the energy spectrum of PNA at different cavity frequencies in a strong coupling situation ($\lambda = 0.05$) (Figure 5.5 (a)). A dispersion of the spectrum with the coupling value for $\omega_{cav} = 0.2$ was also calculated, see Figure 5.5 (b). The geometry of PNA was optimized using DFT with B3LYP and 6-31G+*. The QED calculation was run using only one photonic state.

For this system, the charge-transfer transition is mainly characterized by the transition between HOMO and LUMO, illustrated in Figures 5.4 (b) and (c). In the limit of no coupling we recover the standard CCSD energies (blue) with the photon excitations (red) independently. With increased coupling, the electronic states and photon excited states mix into the polaritons (yellow), creating a superposition between the two states. The polaritons differ in energy and properties compared to standard states. Because of the strong transition dipole moment of the charge transfer state, the Rabi splitting is quite large (1.22 eV) as seen in Figure 5.5 (a). By choosing the frequency and coupling strength of the cavity, the energy levels of PNA can be manipulated. This could be used for instance in photovoltaic devices to align the energy levels of the dye to the conduction band of the semi-conductor. Latini *et al.* have discussed the energy reordering of excitonic energies due to coupling with an optical cavity in 2D semiconductors (transition metal dicalchogenides)[9]. Similarly, for stronger coupling values the order of the excited states energies inverts (Figure 5.5 (b)). The

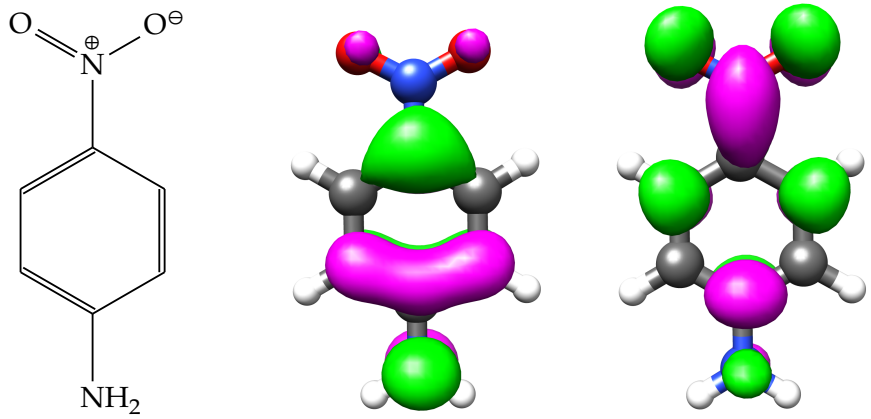

a **b /** HOMO **c /** LUMO

Figure 5.4 / The structure of p-nitroaniline (PNA) is shown in (a). The charge transfer transition of PNA is between HOMO (b) and LUMO (c).

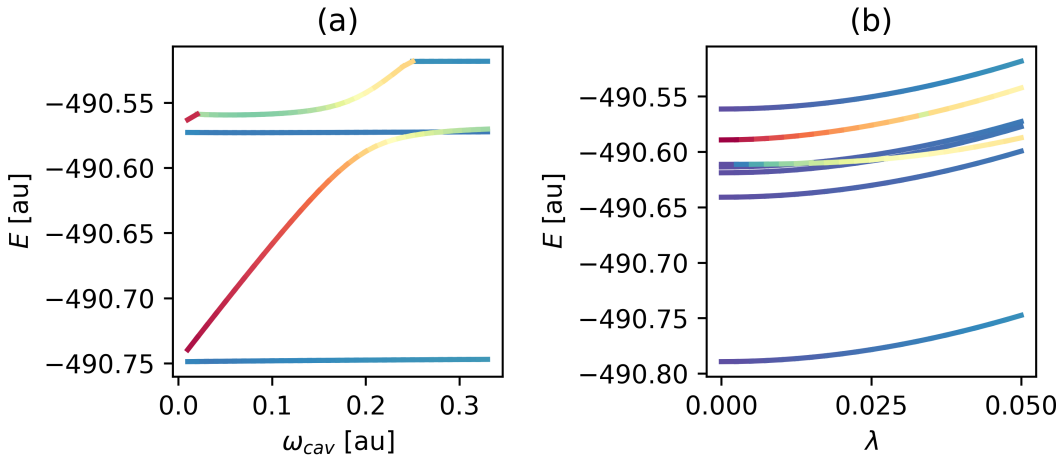

Figure 5.5 / Energy spectrum of p-nitroaniline where blue indicates electronic state, red photon and yellow polariton. (a) The ground state and three excited states of p-nitroanilin (PNA) as a function of the cavity frequency ω_{cav} for strong coupling $\lambda = 0.05$. (b) The ground state and six lowest excited states as a function of the coupling in a resonant cavity $\omega_{cav} = 0.2$.

change in the order of the excited states inside the cavity will cause a change in the photochemistry of the molecule without requiring any modification of the functional groups. The change in the potential energy surfaces can bring the energy barriers up and down, changing the stability of states. This effect has previously been used to stabilize an unstable molecule[52].

Chapter 6

Conclusion and Perspective

Strong light-matter interaction is a new scientific field which has gained popularity during the last decade due to its potential to manipulate and create new properties in molecules without changing the chemical composition. An *ab initio* theory explaining electron-electron and electron-photon correlation is needed to explain quantitatively experimental results as well as inspire new experiments.

For the moment the only reasonable option available to investigate strong light-matter coupling in optical cavities is QED-DFT, in which finding a good exchange-correlation functional is extremely complicated. Another option is QED-FCI, which is accurate but due to the exponentially scaling computational cost, it cannot be applied to realistic systems. In this thesis, we have developed a new methodology based on coupled cluster theory, named QED-CC. QED-CC is able to serve as a middle-ground between QED-DFT and QED-FCI, providing accuracy and efficiency at the same time. Specifically, we have developed two flavors of QED-CC (QED-CCS and QED-CCSD) with different levels of approximation. We tested our approach on prototype systems, but also on realistic molecules, proving the accuracy of the approach. These encouraging results open the way to a big number of further studies that could be investigated using this procedure.

For instance, cavities have been used to inhibit[2], catalyze[3] and induce selectivity[4] in chemical reactions. These effects, introducing some extension to the existent method, could be studied with QED-CC to capture the effects produced by cavities on the chemical reactivity with higher accuracy. We have shown that new potential energy surfaces arise with strong light-matter coupling, which could be used to change the photochemistry of molecules. One application of this would be in photovoltaics, where we could use, as mentioned in previous sections, cavities to align energy levels of the involved materials to improve electron injection processes. It is interesting pointing out also that the effect produced by the cavity is effective also if the involved materials are not in contact with each other.

Vital in comparing theoretical results to experiments is transition dipole moments,

which can be developed from a QED extension of linear response. Building a toolbox of response properties in QED-CC would increase the understanding of what changes the strong light-matter interaction induces. A current limitation with QED-CCSD is that only 1 photon is allowed. The extension from 1 photon to multiple photons and photon modes is straightforward to implement.

Differently from mean-field methods, QED-CC is also able to capture electronic changes in the ground state of the molecular system due to the bi-linear coupling term. This might be used for designing new systems with electronic and reactive properties on demand, as envisioned by Basov *et al*[1].

From our discussion, it is clear that having a tool like QED-CC available opens the way to a huge number of interesting and highly appealing projects that should be investigated. This is also motivated by the fact that cavity QED applied to realistic systems is still in its infancy, and requires investigations already at the fundamental point of view. Several questions still needs to be answered. Why is vibrational strong coupling able modify the reactivity of chemical systems? What happens when chiral light interacts with matter inside a cavity? How do molecules interact through long-range effects from the entangled photons? All of these are completely new directions that could be pursued, and for which QED-CC could represent the reference method of investigation from the theoretical point of view.

Bibliography

1. Basov, D. N., Averitt, R. D. & Hsieh, D. Towards properties on demand in quantum materials. *Nature Materials* **16,** 1077–1088 (2017).
2. Thomas, A. *et al.* Ground-State Chemical Reactivity under Vibrational Coupling to the Vacuum Electromagnetic Field. *Angewandte Chemie - International Edition* **55,** 11462–11466 (2016).
3. Thomas, A. *et al.* Tilting a ground-state reactivity landscape by vibrational strong coupling. *Science* **363,** 615–619 (2019).
4. Ebbesen, T. W. Hybrid Light-Matter States in a Molecular and Material Science Perspective. *Accounts of Chemical Research1* **49,** 2403–2412 (2016).
5. Semenov, A. & Nitzan, A. Electron transfer in confined electromagnetic fields. *The Journal of Chemical Physics* **150,** 174122 (2019).
6. Schäfer, C., Ruggenthaler, M., Appel, H. & Rubio, A. Modification of excitation and charge transfer in cavity quantum-electrodynamical chemistry. *Proceedings of the National Academy of Sciences* **116,** 4883–4892 (2019).
7. Fregoni, J., Granucci, G., Coccia, E., Persico, M. & Corni, S. Manipulating azobenzene photoisomerization through strong light–molecule coupling. *Nature Communications* **9,** 4688 (2018).
8. Byrnes, T., Kim, N. Y. & Yamamoto, Y. Exciton-polariton condensates. *Nature Physics* **10,** 803–813 (2014).
9. Latini, S., Ronca, E., De Giovannini, U., Hübener, H. & Rubio, A. Cavity control of excitons in two-dimensional materials. *Nano Letters* (2019).
10. Sentef, M. A., Ruggenthaler, M. & Rubio, A. Cavity quantum-electrodynamical polaritonically enhanced electron-phonon coupling and its influence on superconductivity. *arXiv* **4,** 1–7 (2018).
11. Cavalleri, A. Photo-induced superconductivity. *Contemporary Physics* **59,** 31–46 (2018).
12. Lindner, N. H., Refael, G. & Galitski, V. Floquet topological insulator in semiconductor quantum wells. *Nature Physics* **7,** 490–495 (2011).
13. Wang, X., Ronca, E. & Sentef, M. A. Cavity Quantum-Electrodynamical Chern Insulator: Route Towards Light-Induced Quantized Anomalous Hall Effect in Graphene. *arXiv* (2019).

14. Delone, N. & Krainov, V. AC Stark shift of atomic energy levels. *Uspekhi Fizicheskih Nauk* **169,** 753 (2008).

15. Basov, D. N., Fogler, M. M. & García De Abajo, F. J. Polaritons in van der Waals materials. *Science* **354** (2016).

16. Dalton, B. J. & Knight, P. L. The standard model in cavity quantum electrodynamics. I. General features of mode functions for a Fabry-Perot cavity. *Journal of Modern Optics* **46,** 1817–1837 (1999).

17. Cummings, F. & Jaynes, E. Comparison of quantum and semiclassical radiation theories with application to the beam maser. *Proceedings of the IEEE* **51,** 89–109 (1963).

18. Chikkaraddy, R. *et al.* Single-molecule strong coupling at room temperature in plasmonic nanocavities. *Nature* **535,** 127–130 (2016).

19. Sun, Z. *et al.* Optical control of roomerature valley polaritons. *Nature Photonics* **11,** 491–496 (2017).

20. Sigle, D. O. *et al.* Monitoring Morphological Changes in 2D Monolayer Semiconductors Using. *ACS Nano* **9,** 825 (2015).

21. Benz, A., Campione, S., Klem, J. F., Sinclair, M. B. & Brener, I. Control of strong light-matter coupling using the capacitance of metamaterial nanocavities. *Nano Letters* **15,** 1959–1966 (2015).

22. Galfsky, T., Gu, J., Narimanov, E. E. & Menon, V. M. Photonic hypercrystals for control of light–matter interactions. *Proceedings of the National Academy of Sciences* **114,** 5125–5129 (2017).

23. Helgaker, T., Jørgensen, P. & Olsen, J. *Molecular Electronic-Structure Theory* (John Wiley & Sons, Ltd, Chichester, UK, 2000).

24. Bauschlicher, C. W. & Taylor, P. R. Benchmark full configuration-interaction calculations on H2O, F, and F-. *The Journal of Chemical Physics* **85,** 2779–2783 (1986).

25. Olsen, J., Jørgensen, P. & Simons, J. Passing the one-billion limit in full configuration-interaction (FCI) calculations. *Chemical Physics Letters* **169,** 463–472 (1990).

26. Larsen, H., Olsen, J., Jørgensen, P. & Christiansen, O. Full configuration interaction benchmarking of coupled-cluster models for the lowest singlet energy surfaces of N2. *Journal of Chemical Physics* **113,** 6677–6686 (2000).

27. Purvis, G. D. & Bartlett, R. J. A full coupled-cluster singles and doubles model: The inclusion of disconnected triples. *The Journal of Chemical Physics* **76,** 1910–1918 (1982).

28. Raghavachari, K., Trucks, G., John A. Pople & Head-Gordon, M. A fifth-order perturbation comparison of electron correlation theories. *Chemical Physics ...* **157,** 479–483 (1989).

29. Parr, R. G. Density Functional Theory. *Annual Review of Physical Chemistry* **34,** 631–656 (1983).

30. Geerlings, P., De Proft, F. & Langenaeker, W. Conceptual Density Functional Theory. *Chemical Reviews* **103,** 1793–1874 (2003).
31. Rivera, N., Flick, J. & Narang, P. Variational theory of nonrelativistic quantum electrodynamics. *Physical Review Letters* **122,** 193603 (2019).
32. Ruggenthaler, M. *et al.* Quantum-electrodynamical density-functional theory: Bridging quantum optics and electronic-structure theory. *Physical Review A - Atomic, Molecular, and Optical Physics* **90,** 012508 (2014).
33. Pellegrini, C., Flick, J., Tokatly, I. V., Appel, H. & Rubio, A. Optimized Effective Potential for Quantum Electrodynamical Time-Dependent Density Functional Theory. *Physical Review Letters* **115,** 093001 (2015).
34. Flick, J., Ruggenthaler, M., Appel, H. & Rubio, A. Kohn–Sham approach to quantum electrodynamical density-functional theory: Exact time-dependent effective potentials in real space. *Proceedings of the National Academy of Sciences* **112,** 15285–15290 (2015).
35. Flick, J., Schäfer, C., Ruggenthaler, M., Appel, H. & Rubio, A. Ab Initio Optimized Effective Potentials for Real Molecules in Optical Cavities: Photon Contributions to the Molecular Ground State. *ACS Photonics* **5,** 992–1005 (2018).
36. Gerry, C. & Knight, P. *Introductory Quantum Optics* (Cambridge University Press, Cambridge, 2004).
37. Stoler, D. Generalized Coherent States. *Physical Review D* **4,** 2309–2312 (1971).
38. Philbin, T. G. Generalized coherent states. *American Journal of Physics* **82,** 742–748 (2014).
39. Pauli, W. & Fierz, M. Zur Theorie der Emission langwelliger Lichtquanten. *Il Nuovo Cimento* **15,** 167–188 (1938).
40. Faisal, F. H. M. *Theory of Multiphoton Processes* (Springer US, Boston, MA, 1987).
41. Bachor, H.-A. *A Guide to Experiments in Quantum Optics* 1st ed. (1998).
42. Hertzog, M., Wang, M., Mony, J. & Börjesson, K. Strong light-matter interactions: A new direction within chemistry. *Chemical Society Reviews* **48,** 937–961 (2019).
43. Garziano, L. *et al.* Multiphoton quantum Rabi oscillations in ultrastrong cavity QED. *Physical Review A* **92,** 063830 (2015).
44. Maciejewski, A. J., Przybylska, M. & Stachowiak, T. Full spectrum of the Rabi model. *Physics Letters A* **378,** 16–20 (2014).
45. Koch, H. & Jørgensen, P. Coupled cluster response functions. *The Journal of Chemical Physics* **93,** 3333–3344 (1990).
46. Pedersen, T. B. & Koch, H. Coupled cluster response functions revisited. *Journal of Chemical Physics* **106,** 8059–8072 (1997).

47. Stanton, J. F. & Bartlett, R. J. The equation of motion coupled-cluster method. A systematic biorthogonal approach to molecular excitation energies, transition probabilities, and excited state properties. *The Journal of Chemical Physics* **98,** 7029–7039 (1993).

48. Rokaj, V., Welakuh, D. M., Ruggenthaler, M. & Rubio, A. Light-matter interaction in the long-wavelength limit: No ground-state without dipole self-energy. *Journal of Physics B: Atomic, Molecular and Optical Physics* **51,** 1–30 (2018).

49. Folkestad, S. D., Kjønstad, E. F. & Koch, H. An efficient algorithm for Cholesky decomposition of electron repulsion integrals. *The Journal of Chemical Physics* **150,** 194112 (2019).

50. Sok, S., Willow, S. Y., Zahariev, F. & Gordon, M. S. Solvent-Induced Shift of the Lowest Singlet $\pi \rightarrow \pi^*$ Charge-Transfer Excited State of p -Nitroaniline in Water: An Application of the TDDFT/EFP1 Method. *The Journal of Physical Chemistry A* **115,** 9801–9809 (2011).

51. Cabral, B. J. C., Coutinho, K. & Canuto, S. A first-principles approach to the dynamics and electronic properties of p-nitroaniline in water. *Journal of Physical Chemistry A* **120,** 3878–3887 (2016).

52. Hutchison, J. A., Schwartz, T., Genet, C., Devaux, E. & Ebbesen, T. W. Modifying Chemical Landscapes by Coupling to Vacuum Fields. *Angewandte Chemie International Edition* **51,** 1592–1596 (2012).

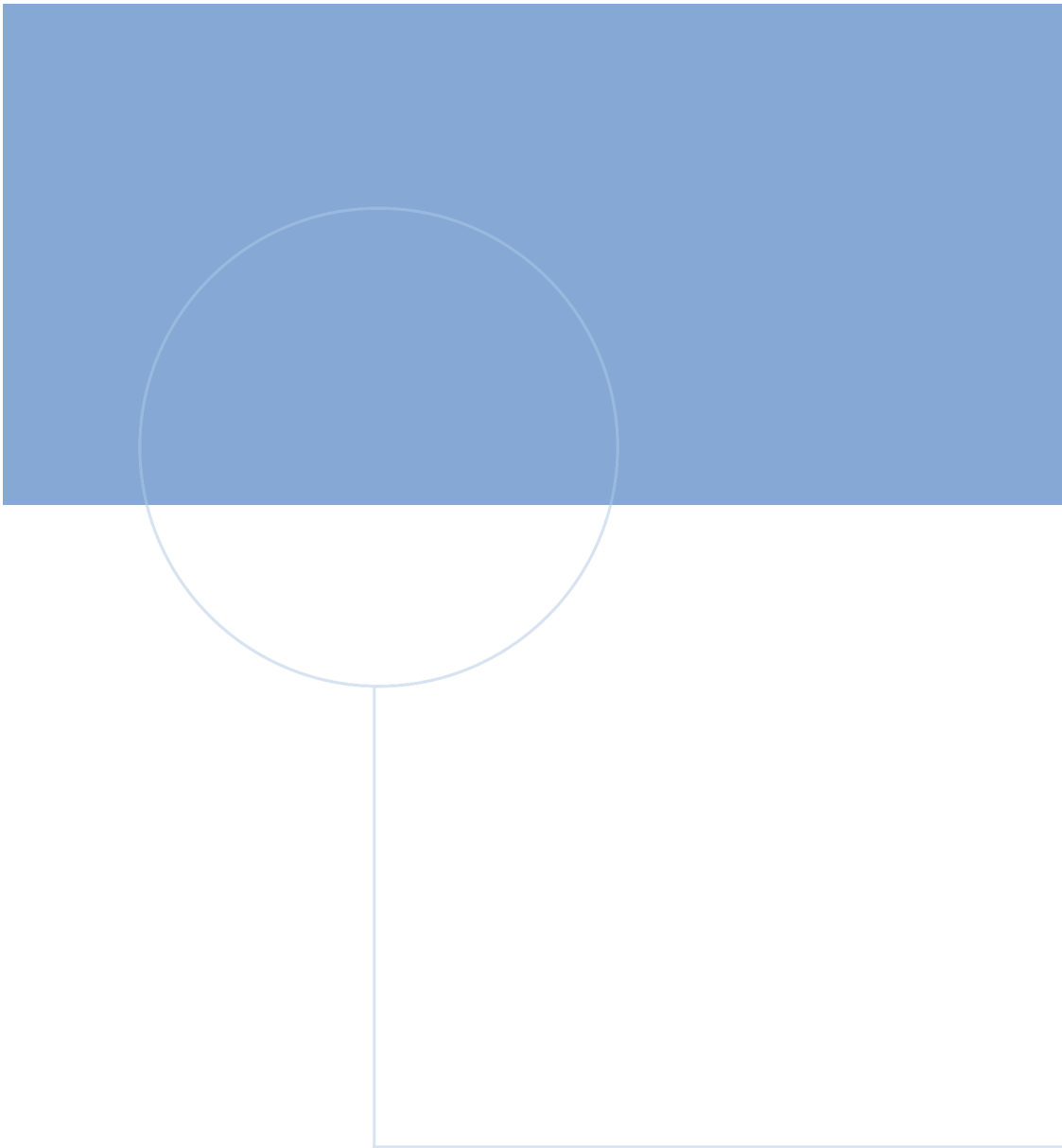

NTNU
Norwegian University of
Science and Technology